HARMONIC ANALYSIS AND SIMULATION
OF
HOMOGENEOUS STOCHASTIC FIELDS

M. Shinozuka[(1)] and T. Harada[(2)]

1986 (1st Edition)
2021(2nd Edition)

1. Renwick Professor of Civil Engineering, Department of Civil Engineering and Engineering Mechanics, Columbia University, New York, NY.

2. Visiting Research Scientist, Department of Civil Engineering and Engineering Mechanics, Columbia University; Professor, Faculty of Engineering, Miyazaki University, Miyazaki, Japan (1986).
Professor Emeritus of University of Miyazaki, Japan (2018).
Email:harada@eerc.co.jp

CONTENTS

1. INTRODUCTION

In this paper, a spectral representation of stochastic fields is given in a form that is convenient for their simulation or digital generation of their sample functions. In a previous paper, Shinozuka and Jan (1972) discussed a simulation technique of multivariate multi-dimensional homogeneous as well as nonhomogeneous processes which represent frozen patterns of stochastic waves propagating in the direction specified by the wave number vector located in the first or last quadrant in an n-dimensional rectangular Cartesian coordinate system for wave numbers. The wave numbers are positive (negative). In this sense, the fields simulated by Shinozuka and Jan are not consistent with the general spectral representation of stochastic processes, although their simulated stochastic fields satisfy the target power spectral density (or correlation) functions. A revised version of the simulation technique was published by Shinozuka (1985) to satisfy this situation. The present paper provides a more detailed analysis in this direction.

The present paper also discusses how time space stochastic processes or stochastic waves, can be characterized within the framework of a second order analysis. Tn this connection, the numerical examples involving seismic array records in Taiwan (SMART-1) are worked out. Finally, brief account is made in this paper as to how the spectral density functions of bi-variate two dimensional stochastic fields or stochastic waves can be estimated from a set of data in a finite region. Although the present study restricts itself to bi-variate two dimensional cases for simplicity, the results may be easily extended to multi-variate multi-dimensional cases.

2. SPECTRAL REPRESENTATION AND SIMULATION OF BI-VARIATE ONE DIMENSIONAL STOCHASTIC FIELDS

2.1 Complex Valued Stochastic Fields

In the harmonic analysis of stochastic fields, it is convenient to consider the fields to be complex-valued. Real-valued stochastic fields can be treated as a special case of complex-valued fields.

The complex stochastic fields $f(x)$ and $g(x)$ can be defined such that

$$\begin{aligned} f(x) &= f^{(1)}(x) + if^{(2)}(x) \\ g(x) &= g^{(1)}(x) + ig^{(2)}(x) \end{aligned} \tag{2.1-1}$$

where is $i = \sqrt{-1}$ the imaginary unit and the functions $f^{(1)}(x), f^{(2)}(x), g^{(1)}(x)$ and $g^{(2)}(x)$ mean real stochastic fields as functions of the space coordinate x. The expected value can be defined as

$$\begin{aligned} E[f(x)] &= E[f^{(1)}(x)] + iE[f^{(2)}(x)] \\ E[g(x)] &= E[g^{(1)}(x)] + iE[g^{(2)}(x)] \end{aligned} \tag{2.1-2}$$

where $E[\bullet]$ means the expectation operator.

If the fields are homogeneous with zero mean;

$$E[f^{(1)}(x)] = E[f^{(2)}(x)] = E[g^{(1)}(x)] = E[g^{(2)}(x)] = 0 \tag{2.1-3}$$

Then, the covariance function matrix can be defined as

$$\boldsymbol{R}(\xi) = \begin{pmatrix} R_{ff}(\xi) & R_{fg}(\xi) \\ R_{gf}(\xi) & R_{gg}(\xi) \end{pmatrix}$$
$$= \begin{pmatrix} E[f(x+\xi)f^*(x)] & E[f(x+\xi)g^*(x)] \\ E[g(x+\xi)f^*(x)] & E[g(x+\xi)g^*(x)] \end{pmatrix} \tag{2.1-4}$$

where $f^*(x)$ denotes the complex conjugate of $f(x)$; $f^*(x) = f^{(1)}(x) - if^{(2)}(x)$. From Eq. (2.1-4), it can be shown that the covariance function satisfies the following condition:

$$R_{jk}(\xi) = R^*_{kj}(-\xi) \tag{2.1-5}$$

where j denotes f or g and so does k; this notation will be used throughout.

The stochastic fields $f(x)$ and $g(x)$ can be represented by the following integrals:

$$f(x) = \int_{-\infty}^{\infty} \mathrm{e}^{i\kappa x} dZ_f(\kappa), \quad g(x) = \int_{-\infty}^{\infty} \mathrm{e}^{i\kappa x} dZ_g(\kappa) \tag{2.1-6}$$

where $dZ_f(\kappa)$ and $dZ_g(\kappa)$ are the orthogonal increments satisfying the following conditions (Yaglom (1962, 1973)):

$$\begin{aligned} & E[dZ_j(\kappa)] = 0 \\ & E[dZ_j(\kappa) dZ^*_k(\kappa')] = \begin{cases} \delta(\kappa - \kappa') dF_{jk}(\kappa') & j \neq k \\ \delta(\kappa - \kappa') \,\mathrm{Re}\; dF_{jk}(\kappa') \\ \mathrm{Im}\; dF_{jk}(\kappa') = 0 & j = k \end{cases} \\ & \frac{dF_{jk}(\kappa)}{d\kappa} = S_{jk}(\kappa) \end{aligned} \tag{2.1-7}$$

where $\delta(\kappa)$ means the delta function and $\mathrm{Re}(\bullet)$ expresses real part. For $\kappa \neq \kappa'$, $\delta(\kappa - \kappa') = 0$ and $\int \delta(\kappa - \kappa') dF_{jk}(\kappa') = dF_{jk}(\kappa)$.

Substitution of Eq. (2.1-6) into Eq. (2.1-4) and use of Eq. (2.1-7) result in

$$\begin{aligned} R_{jk}(\xi) &= E[j(x+\xi)k^*(x)] \\ &= \int_{-\infty}^{\infty}\int_{-\infty}^{\infty} \mathrm{e}^{i\kappa(x+\xi)} \mathrm{e}^{-i\kappa' x} E[dZ_j(\kappa) dZ_k^*(\kappa')] \\ &= \int_{-\infty}^{\infty}\int_{-\infty}^{\infty} \mathrm{e}^{i(\kappa-\kappa')x} \mathrm{e}^{i\kappa\xi} \delta(\kappa - \kappa') dF_{jk}(\kappa') \\ &= \int_{-\infty}^{\infty} \mathrm{e}^{i\kappa\xi} dF_{jk}(\kappa) \end{aligned} \tag{2.1-8}$$

If $dF_{jk}(\kappa)$ is differentiable, then the integral of Eq. (2.1-8) reduces to:

$$R_{jk}(\xi) = \int_{-\infty}^{\infty} \mathrm{e}^{i\kappa\xi} S_{jk}(\kappa) d\kappa \tag{2.1-9a}$$

The inverse transform gives $S_{jk}(\kappa)$ in terms of $R_{jk}(\xi)$:

$$S_{jk}(\kappa) = \frac{1}{2\pi} \int_{-\infty}^{\infty} \mathrm{e}^{-i\kappa\xi} R_{jk}(\xi) d\xi \tag{2.1-9b}$$

Eqs, (2.1-9a) and (2.1-9b) represent the well-known Wiener Khintchine transform pair.

When $j = k$, then Eqs. (2.1-9a) and (2.1-9b) reduce to

$$\begin{aligned} R_{jj}(\xi) &= \int_{-\infty}^{\infty} \mathrm{e}^{i\kappa\xi} S_{jj}(\kappa) d\kappa \\ S_{jj}(\kappa) &= \frac{1}{2\pi} \int_{-\infty}^{\infty} \mathrm{e}^{-i\kappa\xi} R_{jj}(\xi) d\xi \end{aligned} \tag{2.1-10}$$

where $R_{jj}(\xi)$ and $S_{jj}(\kappa)$ are the autocorrelation function and the power spectral density function of $j(x)$ with $R_{jj}(\xi) = R_{jj}(-\xi)$ and $S_{jj}(\kappa) = S_{jj}(-\kappa)$.

2.2 Real Valued Stochastic Fields

Consider that the complex valued increment functions $dF_{jk}(\kappa)$ and $dZ_j(\kappa)$ introduced above are represented in terms of orthogonal increments such that

$$\begin{aligned} dF_{jk}(\kappa) &= \frac{1}{2}(dF_{jk}^{(1)}(\kappa) - idF_{jk}^{(2)}(\kappa)) \\ dZ_j(\kappa) &= \frac{1}{2}(dU_j^{(1)}(\kappa) - idU_j^{(2)}(\kappa)) \end{aligned} \tag{2.2-1}$$

where the functions $dF_{jk}^{(1)}, dF_{jk}^{(2)}, dU_j^{(1)}$ and $dU_j^{(2)}$ are real-valued.

Substitution of Eq. (2.2-1) into Eq. (2.1-7), we obtain the followings;

$$E[dU_j^{(1)}(\kappa)] = E[dU_j^{(2)}(\kappa)] = 0 \tag{2.2-2a}$$

and

$$\begin{aligned} E[dZ_j(\kappa)dZ_k^*(\kappa')] &= \frac{1}{4}\left(\begin{pmatrix} E[dU_j^{(1)}(\kappa)dU_k^{(1)}(\kappa')] + \\ E[dU_j^{(2)}(\kappa)dU_k^{(2)}(\kappa')] \end{pmatrix} + \atop i\begin{pmatrix} E[dU_j^{(1)}(\kappa)dU_k^{(2)}(\kappa')] - \\ E[dU_j^{(2)}(\kappa)dU_k^{(1)}(\kappa')] \end{pmatrix}\right) \\ &= \frac{1}{2}\delta(\kappa - \kappa')(dF_{jk}^{(1)}(\kappa') - idF_{jk}^{(2)}(\kappa')) \end{aligned} \tag{2.2-2b}$$

From Eq. (2.2-2b), the increment real valued functions $dF_{jk}^{(1)}, dF_{jk}^{(2)}, dU_j^{(1)}$ and $dU_j^{(2)}$ must satisfy the following equations;

$$
\begin{aligned}
E[dU_j^{(1)}(\kappa)dU_k^{(1)}(\kappa')] &= E[dU_j^{(2)}(\kappa)dU_k^{(2)}(\kappa')] \\
&= \delta(\kappa-\kappa')dF_{jk}^{(1)}(\kappa') \\
E[dU_j^{(1)}(\kappa)dU_k^{(2)}(\kappa')] &= -E[dU_j^{(2)}(\kappa)dU_k^{(1)}(\kappa')] \\
&= \begin{cases} \delta(\kappa-\kappa')dF_{jk}^{(2)}(\kappa') & j \neq k \\ 0 & j = k \end{cases}
\end{aligned}
\tag{2.2-2c}
$$

Substitution of Eq. (2.2-1) into Eqs. (2.1-6) and (2.1-7) yields the following alternative expressions for $R_{jk}(\xi)$ and $j(x)$:

$$
\begin{aligned}
R_{jk}(\xi) = \frac{1}{2}\int_{-\infty}^{\infty} (\cos\kappa\xi dF_{jk}^{(1)}(\kappa) + \sin\kappa\xi dF_{jk}^{(2)}(\kappa)) \\
+ i\frac{1}{2}\int_{-\infty}^{\infty} (\sin\kappa\xi dF_{jk}^{(1)}(\kappa) - \cos\kappa\xi dF_{jk}^{(2)}(\kappa))
\end{aligned}
\tag{2.2-3a}
$$

and

$$
\begin{aligned}
j(x) = \frac{1}{2}\int_{-\infty}^{\infty} (\cos\kappa\xi dU_j^{(1)}(\kappa) + \sin\kappa\xi dU_j^{(2)}(\kappa)) \\
+ i\frac{1}{2}\int_{-\infty}^{\infty} (\sin\kappa\xi dU_j^{(1)}(\kappa) - \cos\kappa\xi dU_j^{(2)}(\kappa))
\end{aligned}
\tag{2.2-3b}
$$

For real valued stochastic fields, the imaginary parts of $R_{jk}(\xi)$ and $j(x)$ in the above equations must be zero. This requires that,

$$
\begin{aligned}
dF_{jk}^{(1)}(-\kappa) = dF_{jk}^{(1)}(\kappa), \quad dF_{jk}^{(2)}(-\kappa) = -dF_{jk}^{(2)}(\kappa) \\
dU_j^{(1)}(-\kappa) = dU_j^{(1)}(\kappa), \quad dU_j^{(2)}(-\kappa) = -dU_j^{(2)}(\kappa)
\end{aligned}
\tag{2.2-4}
$$

Eq. (2.2-4) implies that the real part of $dF_{jk}(\kappa)$ and $dZ_j(\kappa)$ are even functions of wave number, while their imaginary parts are odd functions of wave number. Therefore, for real valued stochastic fields, the complex valued increment functions $dF_{jk}(\kappa)$ and $dZ_j(\kappa)$ must satisfy the following conditions:

$$
\begin{aligned}
&dF_{jk}(-\kappa) = dF_{jk}^{*}(\kappa) \\
&dZ_{j}(-\kappa) = dZ_{j}^{*}(\kappa)
\end{aligned}
\tag{2.2-5}
$$

Using the above conditions, Eqs. (2.2-2) and (2.2-3) reduce to

$$
R_{jk}(\xi) = R_{jk}^{(1)}(\xi) = \int_0^\infty (\cos\kappa\xi dF_{jk}^{(1)}(\kappa) + \sin\kappa\xi dF_{jk}^{(2)}(\kappa)) \tag{2.2-6}
$$

and

$$
j(x) = j^{(1)}(x) = \int_0^\infty (\cos\kappa x dU_{j}^{(1)}(\kappa) + \sin\kappa x dU_{j}^{(2)}(\kappa)) \tag{2.2-7}
$$

It is not hard to derive Eq. (2.2-6) from Eq. (2.27) in conjunction with Eq. (2.2-2c). In fact,

$$
\begin{aligned}
R_{jk}^{(1)}(\xi) &= E[j^{(1)}(x+\xi)k^{(1)}(x)] \\
&= \int_0^\infty\int_0^\infty E\left[\begin{matrix}\begin{pmatrix}\cos\kappa(x+\xi)\cos\kappa x dU_{j}^{(1)}(\kappa) + \\ \sin\kappa(x+\xi)\sin\kappa x dU_{j}^{(2)}(\kappa)\end{pmatrix}\times \\ \cos\kappa' x dU_{k}^{(1)}(\kappa') + \sin\kappa' x dU_{k}^{(2)}(\kappa')\end{matrix}\right] \\
&= \int_0^\infty \begin{pmatrix}\begin{pmatrix}\cos\kappa(x+\xi)\cos\kappa x + \\ \sin\kappa(x+\xi)\sin\kappa x\end{pmatrix} dF_{jk}^{(1)}(\kappa) + \\ \begin{pmatrix}\sin\kappa(x+\xi)\cos\kappa x - \\ \cos\kappa(x+\xi)\sin\kappa x\end{pmatrix} dF_{jk}^{(2)}(\kappa)\end{pmatrix} \\
&= \int_0^\infty (\cos\kappa\xi dF_{jk}^{(1)}(\kappa) + \sin\kappa\xi dF_{jk}^{(2)}(\kappa))
\end{aligned}
\tag{2.2-8}
$$

Especially when $j = k$, then from Eqs. (2.2-6) and (2.2-2c),

$$
R_{jj}^{(1)}(\xi) = R_{jj}^{(1)}(-\xi), \quad dF_{jj}^{(2)}(\kappa) = 0 \tag{2.2-9}
$$

Hence, Eq. (2.2-6) reduce to

$$
R_{jj}^{(1)}(\xi) = \int_0^\infty \cos\kappa\xi dF_{jj}^{(1)}(\kappa) \tag{2.2-10}
$$

If $dF_{jj}^{(1)}(\kappa)$ is continuous, the power spectral density function $S_{ff}(\kappa)$ can be defined from Eq. (2.1-7) such as

$$\frac{dF_{jj}(\kappa)}{d\kappa} = \frac{1}{2}\frac{dF_{jj}^{(1)}(\kappa)}{d\kappa} = S_{jj}(\kappa) \to dF_{jj}^{(1)}(\kappa) = 2S_{jj}(\kappa)d\kappa \tag{2.2-11}$$

Substituting Eq. (2.2-11) into Eq. (2.2-10), we obtain

$$R_{jj}^{(1)}(\xi) = 2\int_0^\infty \cos\kappa\xi S_{jj}(\kappa)d\kappa \tag{2.2-12a}$$

The inverse transform gives $S_{jj}(\kappa)$ as

$$S_{jj}(\kappa) = \frac{1}{\pi}\int_0^\infty \cos\kappa\xi R_{jj}^{(1)}(\xi)d\xi \tag{2.2-12b}$$

From Eqs. (2.2-9) and (2.2-12b), $R_{jj}^{(1)}(\xi)$ and $S_{jj}(\kappa)$ are even functions, then Eqs. (2.2-12a) and (2.2-12b) can be also expressed as

$$\begin{aligned} R_{jj}^{(1)}(\xi) &= \int_{-\infty}^{\infty} \cos\kappa\xi S_{jj}(\kappa)d\kappa \\ S_{jj}(\kappa) &= \frac{1}{2\pi}\int_{-\infty}^{\infty} \cos\kappa\xi R_{jj}^{(1)}(\xi)d\xi \end{aligned} \tag{2.2-13}$$

It is noted here that the above equation is the real part of the Wiener Khintchine transform pair of Eq. (2.1-10).

2.3 Simulation Method

We now consider the simulation method of the homogeneous stochastic fields $f(x)$ and $g(x)$ under the condition that the power spectral density function $S_{jk}(\kappa)$ is specified such that

$$\boldsymbol{S}(\kappa)=\begin{pmatrix} S_{ff}(\kappa) & S_{fg}(\kappa) \\ S_{gf}(\kappa) & S_{gg}(\kappa) \end{pmatrix}, \quad S_{gf}(\kappa)=S^*_{fg}(\kappa) \tag{2.3-1}$$

Since the power spectral density function matrix constitutes the Hermitian and non-negative definite matrix (Yaglom (1962)), Eq. (2.3-1) can be decomposed as

$$\begin{pmatrix} a_{11} & 0 \\ a_{21} & a_{22} \end{pmatrix}\begin{pmatrix} a^*_{11} & a^*_{21} \\ 0 & a^*_{22} \end{pmatrix}=\begin{pmatrix} |a_{11}|^2 & a_{11}a^*_{21} \\ a_{21}a^*_{11} & |a_{21}|^2+|a_{22}|^2 \end{pmatrix} \tag{2.3-2}$$

where a_{jk} can be obtained by equating Eq. (2.3-1) with Eq. (2.3-2) such that

$$a_{11}=|a_{11}|\,\mathrm{e}^{i\psi_1(\kappa)}=\sqrt{S_{ff}(\kappa)}\,\mathrm{e}^{i\psi_1(\kappa)}$$

$$a_{21}=|a_{21}|\,\mathrm{e}^{i\alpha_{21}(\kappa)}=\frac{|S_{fg}(\kappa)|}{\sqrt{S_{ff}(\kappa)}}\mathrm{e}^{i(\psi_1(\kappa)+\alpha_{21}(\kappa))} \tag{2.3-3a}$$

$$a_{22}=|a_{22}|\,\mathrm{e}^{i\psi_2(\kappa)}=\sqrt{\frac{S_{ff}(\kappa)S_{gg}(\kappa)-|S_{fg}(\kappa)|^2}{S_{ff}(\kappa)}}\,\mathrm{e}^{i\psi_2(\kappa)}$$

(2.3-8) where $\psi_1(\kappa)$ and $\psi_2(\kappa)$ are arbitrary phase angles and

$$\alpha_{21}(\kappa)=\tan^{-1}\left(\frac{\mathrm{Im}(S_{fg}(\kappa))}{\mathrm{Re}(S_{fg}(\kappa))}\right) \tag{2.3-3b}$$

On the other hand, the covariance of the orthogonal increment $dZ_j(\kappa)$ is given by Eq. (2.1-7), that is

$$\begin{aligned} E[dZ_f(\kappa)dZ^*_f(\kappa)] &= S_{ff}(\kappa)d\kappa \\ E[dZ_f(\kappa)dZ^*_g(\kappa)] &= S_{fg}(\kappa)d\kappa \\ E[dZ_g(\kappa)dZ^*_g(\kappa)] &= S_{gg}(\kappa)d\kappa \end{aligned} \tag{2.3-4}$$

Comparison of Eqs. (2.3-2) and (2.3-4) motivates the introduction of a new definition for the orthogonal increments $dZ_f(\kappa)$ and $dZ_g(\kappa)$ to efficiently express the orthogonal increments in terms of the power spectral density functions as follows:

$$\begin{aligned} dZ_f(\kappa) &= dZ_{ff}(\kappa) \\ dZ_g(\kappa) &= dZ_{gf}(\kappa) + dZ_{gg}(\kappa) \end{aligned} \tag{2.3-5a}$$

where

$$E[dZ_{ff}(\kappa)dZ_{gg}^*(\kappa)] = E[dZ_{gf}(\kappa)dZ_{gg}^*(\kappa)] = 0 \tag{2.3-5b}$$

and similarly

$$\begin{aligned} dZ_f(\kappa) &= \frac{1}{2}(dU_{ff}^{(1)}(\kappa) - idU_{ff}^{(2)}(\kappa)) \\ dZ_g(\kappa) &= \frac{1}{2}(dU_{gf}^{(1)}(\kappa) - idU_{gf}^{(2)}(\kappa)) + \frac{1}{2}(dU_{gg}^{(1)}(\kappa) - idU_{gg}^{(2)}(\kappa)) \end{aligned} \tag{2.3-5c}$$

where $dU_{jk}^{(1)}(\kappa)$ and $dU_{jk}^{(2)}(\kappa)$ are real valued.

Substitution of Eq. (2.3-5a) into Eq. (2.3-4) and taking into account Eq. (2.3-5b) yields the following equation as

$$\begin{aligned} &\begin{pmatrix} E[dZ_f(\kappa)dZ_f^*(\kappa)] & E[dZ_f(\kappa)dZ_g^*(\kappa)] \\ E[dZ_g(\kappa)dZ_f^*(\kappa)] & E[dZ_g(\kappa)dZ_g^*(\kappa)] \end{pmatrix} = \\ &\begin{pmatrix} E[| dZ_{ff}(\kappa) |^2] & E[dZ_{ff}(\kappa)dZ_{gf}^*(\kappa)] \\ E[dZ_{gf}(\kappa)dZ_{ff}^*(\kappa)] & E[| dZ_{gf}(\kappa) |^2 + | dZ_{gg}(\kappa) |^2] \end{pmatrix} \end{aligned} \tag{2.3-6}$$

Comparing Eq. (2.3-2) with Eq. (2.3-6), the orthogonal increments an be obtained such that

$$\begin{aligned} dZ_{ff}(\kappa) &= | a_{11} | \sqrt{d\kappa}\, \mathrm{e}^{i\psi_1(\kappa)} \\ dZ_{gf}(\kappa) &= | a_{21} | \sqrt{d\kappa}\, \mathrm{e}^{i(\psi_1(\kappa)+\alpha_{21}(\kappa))} \\ dZ_{gf}(\kappa) &= | a_{22} | \sqrt{d\kappa}\, \mathrm{e}^{i\psi_2(\kappa)} \end{aligned} \tag{2.3-7}$$

also, taking into account Eq. (2.3-5c),

$$\begin{aligned}
dU_{ff}^{(1)}(\kappa) &= 2 \mid a_{11} \mid \sqrt{d\kappa} \cos \psi_1(\kappa) \\
dU_{ff}^{(2)}(\kappa) &= -2 \mid a_{11} \mid \sqrt{d\kappa} \sin \psi_1(\kappa) \\
\\
dU_{gf}^{(1)}(\kappa) &= 2 \mid a_{21} \mid \sqrt{d\kappa} \cos(\psi_1(\kappa)+\alpha_{21}(\kappa)) \\
dU_{gf}^{(2)}(\kappa) &= -2 \mid a_{21} \mid \sqrt{d\kappa} \sin(\psi_1(\kappa)+\alpha_{21}(\kappa)) \\
\\
dU_{gg}^{(1)}(\kappa) &= 2 \mid a_{22} \mid \sqrt{d\kappa} \cos \psi_2(\kappa) \\
dU_{gg}^{(2)}(\kappa) &= -2 \mid a_{22} \mid \sqrt{d\kappa} \sin \psi_2(\kappa)
\end{aligned} \tag{2.3-8}$$

In Eqs. (2.3-7) and (2.3-8), the arbitrary phase angle $\psi_1(\kappa)$ and $\psi_2(\kappa)$ must be appropriate random functions so that the orthogonal increment $dZ_j(\kappa)$ satisfy the orthogonal conditions as given in Eqs. (2.1-7) or (2.2-2c). If we choose independent random phases uniformly distributed between 0 and 2π for $\psi_1(\kappa)$ and $\psi_2(\kappa)$, it is easy to show that Eqs. (2.3-7) and (2.3-8) satisfy Eqs. (2.1-7) or (2.2-2c), respectively.

From Eqs. (2.2-7), (2.3-3) and (2.3-8), the real valued stochastic fields $f^{(1)}(x)$ and $g^{(1)}(x)$ can be expressed as

$$f^{(1)}(x) = \int_0^\infty 2 \mid a_{11} \mid \sqrt{d\kappa} \cos(\kappa x + \psi_1(\kappa)) \tag{2.3-9a}$$

and

$$\begin{aligned}
g^{(1)}(x) = &\int_0^\infty 2 \mid a_{21} \mid \sqrt{d\kappa} \cos(\kappa x + \psi_1(\kappa)+\alpha_{21}(\kappa)) \\
&+\int_0^\infty 2 \mid a_{22} \mid \sqrt{d\kappa} \cos(\kappa x + \psi_2(\kappa))
\end{aligned} \tag{2.3-9b}$$

The integrals mean, for $d\kappa \to 0$ and $\kappa_n = nd\kappa$

$$f^{(1)}(x) = \sum_{n=1}^{N} 2\,|\,a_{11}\,|\,\sqrt{d\kappa}\cos(\kappa_n x + \psi_{1n}(\kappa)) \tag{2.3-10a}$$

and

$$\begin{aligned} g^{(1)}(x) = \sum_{n=1}^{N} & 2\,|\,a_{21}\,|\,\sqrt{d\kappa}\cos(\kappa_n x + \psi_{1n}(\kappa_n) + \alpha_{21}(\kappa_n)) \\ & + 2\,|\,a_{22}\,|\,\sqrt{d\kappa}\cos(\kappa_n x + \psi_{2n}(\kappa_n)) \end{aligned} \tag{2.3-10b}$$

where

$$\begin{aligned} |\,a_{11}\,| &= \sqrt{S_{ff}(\kappa)} \\ |\,a_{21}\,| &= \frac{|\,S_{fg}(\kappa)\,|}{\sqrt{S_{ff}(\kappa)}} \\ |\,a_{22}\,| &= \sqrt{\frac{S_{ff}(\kappa)S_{gg}(\kappa) - |\,S_{fg}(\kappa)\,|^2}{S_{ff}(\kappa)}} \end{aligned} \tag{2.3-10c}$$

Equation (2.3-10) is identical to tha used by Shinozuka and Jan (1972). As shown by them, making use of the FFT (Fast Fourier Transform) technique in the summations appearing in Eq. (2.3-10) drastically reduces the computing time.

3. SPECTRAL REPRESENTATION OF BI-VARIATE TWO-DIMENSIONAL STOCHASTIC FIELDS

The previous procedure described in Chapter 2 can be directly used for the bi-variate two-dimensional case. Almost all the equation in Chapter 3 and 4 are similar, but the equations for real valued fields are quite different. This difference is also quite important in the simulation of real valued stochastic fields as explained in the numerical examples in Chapter 6. To explained the difference, a similar procedure and equation are provided.

3.1 Complex Valued Stochastic Fields

The complex stochastic fields $f(x,y)$ and $g(x,y)$ can be defined as

$$\begin{aligned} f(x,y) &= f^{(1)}(x,y) + if^{(2)}(x,y) \\ g(x,y) &= g^{(1)}(x,y) + ig^{(2)}(x,y) \end{aligned} \tag{3.1-1}$$

where $i = \sqrt{-1}$, the functions $f^{(1)}(x,y)$, $f^{(2)}(x,y)$, $g^{(1)}(x,y)$ and $g^{(2)}(x,y)$ are the real valued stochastic fields, and x,y denote real coordinates. The mean can be defined as

$$\begin{aligned} E[f(x,y)] &= E[f^{(1)}(x,y)] + iE[f^{(2)}(x,y)] \\ E[g(x,y)] &= E[g^{(1)}(x,y)] + iE[g^{(2)}(x,y)] \end{aligned} \tag{3.1-2}$$

where $E[\bullet]$ is the expectation operator.

Now suppose that the fields are homogeneous stochastic fields with zero mean. Then, the covariance function of the fields can be defined in matrix form such that

$$\boldsymbol{R}(\xi_x,\xi_y)=\begin{pmatrix} R_{ff}(\xi_x,\xi_y) & R_{fg}(\xi_x,\xi_y) \\ R_{gf}(\xi_x,\xi_y) & R_{gg}(\xi_x,\xi_y) \end{pmatrix}$$
$$=\begin{pmatrix} E[f(x+\xi_x,y+\xi_y)f^*(x,y)] & E[f(x+\xi_x,y+\xi_y)g^*(x,y)] \\ E[g(x+\xi_x,y+\xi_y)f^*(x,y)] & E[g(x+\xi_x,y+\xi_y)g^*(x,y)] \end{pmatrix} \tag{3.1-3}$$

where $f^*(x,y)=f^{(1)}(x,y)-if^{(2)}(x,y)$ denotes the complex conjugate of $f(x,y)$. Thus

$$R_{jk}(\xi_x,\xi_y)=R_{kj}^*(-\xi_x,-\xi_y),\quad j,k=f,g \tag{3.1-4}$$

that is, the covariance matrix for bi-variate stochastic fields constitutes Hermitian. In particular, the variances of the diagonal term are real and positive, that is,

$$\begin{aligned}\mathrm{Var}[f]&=R_{ff}(0)=E[f(x,y)f^*(x,y)]\\&=E[(f^{(1)}(x,y))^2+(f^{(2)}(x,y))^2]\\ \mathrm{Var}[g]&=R_{gg}(0)=E[g(x,y)g^*(x,y)]\\&=E[(g^{(1)}(x,y))^2+(g^{(2)}(x,y))^2]\end{aligned} \tag{3.1-5}$$

It can be shown for the homogeneous stochastic fields $f(x,y)$ and $g(x,y)$, that the covariance function $R_{jk}(\xi_x,\xi_y),(j,k=f,g)$ can always be represented as follows (Yaglom (1962)):

$$R_{jk}(\xi_x,\xi_y)=\int_{-\infty}^{\infty}\int_{-\infty}^{\infty}\mathrm{e}^{i(\kappa_x\xi_x+\kappa_y\xi_y)}dF_{jk}(\kappa_x,\kappa_y) \tag{3.1-6}$$

and the fields themselves can be represented as

$$
\begin{aligned}
f(x,y) &= \int_{-\infty}^{\infty}\int_{-\infty}^{\infty} \mathrm{e}^{i(\kappa_x x+\kappa_y y)} dZ_f(\kappa_x,\kappa_y) \\
g(x,y) &= \int_{-\infty}^{\infty}\int_{-\infty}^{\infty} \mathrm{e}^{i(\kappa_x x+\kappa_y y)} dZ_g(\kappa_x,\kappa_y)
\end{aligned}
\tag{3.1-7}
$$

where the integral means the Fourier Stieljes integral standing for the limit, for instance, for the integral of Eq. (3.1-7),

$$
\begin{aligned}
f(x,y) &= \lim_{\substack{a\to\infty \\ b\to\infty}} \int_{-a}^{a}\int_{-b}^{b} \mathrm{e}^{i(\kappa_x x+\kappa_y y)} dZ_f(\kappa_x,\kappa_y) \\
&= \lim_{\substack{a\to\infty \\ b\to\infty}} \lim_{\substack{d\kappa_x\to 0 \\ d\kappa_y\to 0}} \sum_{n=-N}^{N}\sum_{m=-M}^{M} \mathrm{e}^{i(\kappa_{xn} x+\kappa_{ym} y)} dZ_f(\kappa_{xn},\kappa_{ym})
\end{aligned}
\tag{3.1-8a}
$$

where the complex discrete orthogonal increment is defined by all the combination of wave numbers such that

$$
\begin{aligned}
dZ_f(\kappa_{xn},\kappa_{ym}) &= \Big[Z_f(\kappa_{xn},\kappa_{ym})\Big]_{\kappa_{xn},\kappa_{ym}}^{\kappa_{xn}+d\kappa_x,\kappa_{ym}+d\kappa_y} \\
&= Z_f(\kappa_{xn}+d\kappa_x,\kappa_{ym}+d\kappa_y) - Z_f(\kappa_{xn}+d\kappa_x,\kappa_{ym}) \\
&\quad - Z_f(\kappa_{xn},\kappa_{ym}+d\kappa_y) + Z_f(\kappa_{xn},\kappa_{ym})
\end{aligned}
\tag{3.1-8b}
$$

and the summation is over all the subjects appearing in the partition as shown in Fig. 3.1-1.

$$
\begin{aligned}
&-a = \kappa_{x-N} < \cdots \kappa_{xn} \cdots < \kappa_{xN} = a \\
&-b = \kappa_{y-M} < \cdots \kappa_{ym} \cdots < \kappa_{yM} = b \\
&d\kappa_x = \kappa_{xn} - \kappa_{xn-1}, \quad d\kappa_y = \kappa_{ym} - \kappa_{ym-1}
\end{aligned}
\tag{3.1-8c}
$$

The function $F_{jk}(\kappa_x,\kappa_y)$ which is a non-negative and non-decreasing function is called the spectral function of the fields $f(x,y)$ and $g(x,y)$. When the function $F_{jk}(\kappa_x,\kappa_y)$ is continuous, its derivative is called the spectral density function $S_{jk}(\kappa_x,\kappa_y)$, that is

$$S_{jk}(\kappa_x,\kappa_y) = \frac{\partial^2 F_{jk}(\kappa_x,\kappa_y)}{\partial\kappa_x\partial\kappa_y} \tag{3.1-9}$$

Then, the Fourier Stieltjes integral of Eq. (3.1-7) reduces to the Fourier integral as

$$R_{jk}(\xi_x,\xi_y) = \int_{-\infty}^{\infty}\int_{-\infty}^{\infty} \mathrm{e}^{i(\kappa_x\xi_x+\kappa_y\xi_y)} S_{jk}(\kappa_x,\kappa_y)d\kappa_x d\kappa_y \tag{3.1-10a}$$

The inverse transformation yields the spectral density function as

$$S_{jk}(\kappa_x,\kappa_y) = \frac{1}{(2\pi)^2}\int_{-\infty}^{\infty}\int_{-\infty}^{\infty} \mathrm{e}^{-i(\kappa_x\xi_x+\kappa_y\xi_y)} R_{jk}(\xi_x,\xi_y)d\xi_x d\xi_y \tag{3.1-10b}$$

Equations (3.1-6a) and (3.1-6b) are the Wiener Kintchine relationships.

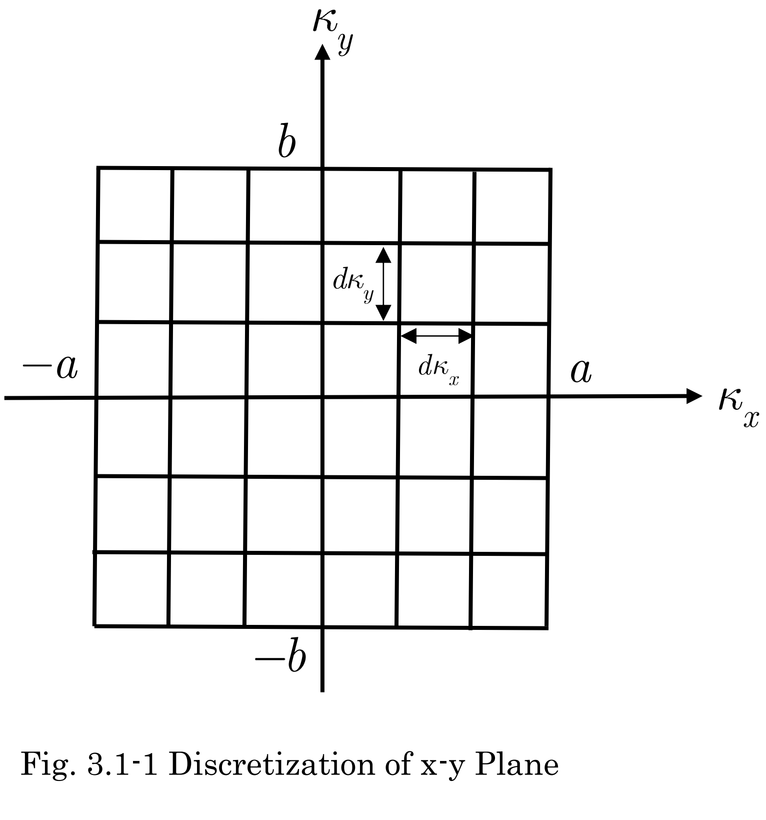

Fig. 3.1-1 Discretization of x-y Plane

Turning to the representations of stochastic fields given by Eq. (3.1-7), these representations imply that $f(x,y)$ and $g(x,y)$ can be written as the sum of many elementary waves $\exp[i(\kappa_x x+\kappa_y y)]$ with complex orthogonal random amplitudes $dZ_f(\kappa_x,\kappa_y)$ and $dZ_g(\kappa_x,\kappa_y)$, respectively. The orthogonal random amplitude is generally called the orthogonal increment which is defined as follows and satisfies the following conditions:

$$
\begin{aligned}
&E[dZ_j(\kappa_x,\kappa_y)]=0\\
&E[dZ_j(\kappa_x,\kappa_y)dZ_k^*(\kappa_x',\kappa_y')]=\\
&\qquad\begin{cases}\delta(\kappa_x-\kappa_x')\delta(\kappa_y-\kappa_y')dF_{jk}(\kappa_x',\kappa_y') & j\neq k\\ \delta(\kappa_x-\kappa_x')\delta(\kappa_y-\kappa_y')\,\mathrm{Re}\ dF_{jk}(\kappa_x',\kappa_y') & j=k\end{cases}\\
&\frac{\partial^2 F_{jk}(\kappa_x,\kappa_y)}{\partial\kappa_x\partial\kappa_y}=S_{jk}(\kappa_x,\kappa_y)
\end{aligned}
\tag{3.1-11a}
$$

where $\delta(\kappa_x,\kappa_y)=\delta(\kappa_x)\delta(\kappa_y)$ means the delta function with the conditions:

$$
\begin{aligned}
&\delta(\kappa_x-\kappa_x')\delta(\kappa_y-\kappa_y')=\begin{cases}\infty & \kappa_x=\kappa_x',\kappa_y=\kappa_y'\\ 0 & \kappa_x\neq\kappa_x',\kappa_y\neq\kappa_y'\end{cases}\\
&\iint\delta(\kappa_x-\kappa_x')\delta(\kappa_y-\kappa_y')dF_{jk}(\kappa_x',\kappa_y')=dF_{jk}(\kappa_x,\kappa_y)
\end{aligned}
\tag{3.1-11b}
$$

and $\mathrm{Re}(\bullet)$ expresses real part.

Due to Eqs. (3.1-11a) and (3.1-11b) (orthogonal conditions), it is easily confirmed that the covariance function is given by Eq. (3.1-6). In fact,

$$
\begin{aligned}
R_{jk}(\xi_x,\xi_y)&=E[j(x+\xi_x,y+\xi_y)k^*(x,y)]\\
&=\int_{-\infty}^{\infty}\int_{-\infty}^{\infty}\int_{-\infty}^{\infty}\int_{-\infty}^{\infty}\begin{pmatrix}\mathrm{e}^{i[\kappa_x(x+\xi_x)+\kappa_y(y+\xi_y)]}\mathrm{e}^{-i[\kappa_x'x+\kappa_y'y]}\times\\ E[dZ_j(\kappa_x,\kappa_y)dZ_k^*(\kappa_x',\kappa_y')]\end{pmatrix}\\
&=\int_{-\infty}^{\infty}\int_{-\infty}^{\infty}\mathrm{e}^{i(\kappa_x\xi_x+\kappa_y\xi_y)}dF_{jk}(\kappa_x,\kappa_y)
\end{aligned}
\tag{3.1-12}
$$

3.2 Real Valued Stochastic Fields

Suppose the complex valued spectral distribution function $F_{jk}(\kappa_x,\kappa_y)$ and the orthogonal function $Z_j(\kappa_x,\kappa_y)$ are represented in terms of the increment such that

$$\begin{aligned} dF_{jk}(\kappa_x,\kappa_y) &= \frac{1}{2}\ dF_{jk}^{(1)}(\kappa_x,\kappa_y) - idF_{jk}^{(2)}(\kappa_x,\kappa_y) \\ dZ_j(\kappa_x,\kappa_y) &= \frac{1}{2}\ dU_j^{(1)}(\kappa_x,\kappa_y) - idU_j^{(2)}(\kappa_x,\kappa_y) \end{aligned} \tag{3.2-1}$$

where $dF_{jk}^{(1)}$ and $dF_{jk}^{(2)}$ are the real valued spectral distribution functions associated with the real and imaginary parts of dF_{jk}. The functions $dU_j^{(1)}$ and $dU_j^{(2)}$ are also the real valued increments associated with the real and imaginary parts of dZ_j.

Substitution of Eq. (3.2-1) into Eqs. (3.1-6) and (3.1-7) yields alternative expressions for $R_{jk}(\xi_x,\xi_y)$ and $j(x,y)$ such that

$$\begin{aligned} R_{jk}(\xi_x,\xi_y) &= \frac{1}{2}\int_{-\infty}^{\infty}\int_{-\infty}^{\infty}\left(\begin{array}{l}\cos(\kappa_x\xi_x+\kappa_y\xi_y)dF_{jk}^{(1)}(\kappa_x,\kappa_y)+\\ \sin(\kappa_x\xi_x+\kappa_y\xi_y)dF_{jk}^{(2)}(\kappa_x,\kappa_y)\end{array}\right) \\ &+i\frac{1}{2}\int_{-\infty}^{\infty}\int_{-\infty}^{\infty}\left(\begin{array}{l}\sin(\kappa_x\xi_x+\kappa_y\xi_y)dF_{jk}^{(1)}(\kappa_x,\kappa_y)-\\ \cos(\kappa_x\xi_x+\kappa_y\xi_y)dF_{jk}^{(2)}(\kappa_x,\kappa_y)\end{array}\right) \end{aligned} \tag{3.2-2}$$

and the fields $f(x,y)$ and $g(x,y)$ are for $j=f,g$,

$$j(x,y)=\frac{1}{2}\int_{-\infty}^{\infty}\int_{-\infty}^{\infty}\begin{pmatrix}\cos(\kappa_x x+\kappa_y y)dU_j^{(1)}(\kappa_x,\kappa_y)+\\ \sin(\kappa_x x+\kappa_y y)dU_j^{(2)}(\kappa_x,\kappa_y)\end{pmatrix}$$

$$+i\frac{1}{2}\int_{-\infty}^{\infty}\int_{-\infty}^{\infty}\begin{pmatrix}\sin(\kappa_x x+\kappa_y y)dU_j^{(1)}(\kappa_x,\kappa_y)-\\ \cos(\kappa_x x+\kappa_y y)dU_j^{(2)}(\kappa_x,\kappa_y)\end{pmatrix} \tag{3.2-3}$$

For real valued stochastic fields, the imaginary parts of $R_{jk}(\xi_x,\xi_y)$ and $j(x,y)$ given by Eqs. (3.2-2) and (3.2-3) must be zero. This requires the conditions as follows:

$$dF_{jk}^{(1)}(-\kappa_x,-\kappa_y)=dF_{jk}^{(1)}(\kappa_x,\kappa_y),\ dF_{jk}^{(1)}(-\kappa_x,\kappa_y)=dF_{jk}^{(1)}(\kappa_x,-\kappa_y)$$

$$dF_{jk}^{(2)}(-\kappa_x,-\kappa_y)=-dF_{jk}^{(2)}(\kappa_x,\kappa_y),\ dF_{jk}^{(2)}(-\kappa_x,\kappa_y)=-dF_{jk}^{(2)}(\kappa_x,-\kappa_y)$$

$$dU_j^{(1)}(-\kappa_x,-\kappa_y)=dU_j^{(1)}(\kappa_x,\kappa_y),\ dU_j^{(1)}(-\kappa_x,\kappa_y)=dU_j^{(1)}(\kappa_x,-\kappa_y)$$

$$dU_j^{(2)}(-\kappa_x,-\kappa_y)=-dU_j^{(2)}(\kappa_x,\kappa_y),\ dU_j^{(2)}(-\kappa_x,\kappa_y)=-dU_j^{(2)}(\kappa_x,-\kappa_y)$$

(3.2-4)

Above equations yield the conditions for $dF_{jk}(\kappa_x,\kappa_y)$ and $dZ_j(\kappa_x,\kappa_y)$:

$$\begin{aligned}dF_{jk}(-\kappa_x,-\kappa_y)&=dF_{jk}^*(\kappa_x,\kappa_y)\\ dF_{jk}(-\kappa_x,\kappa_y)&=dF_{jk}^*(\kappa_x,-\kappa_y)\end{aligned} \tag{3.2-5a}$$

and

$$\begin{aligned}dZ_j(-\kappa_x,-\kappa_y)&=dZ_j^*(\kappa_x,\kappa_y)\\ dZ_j(-\kappa_x,\kappa_y)&=dZ_j^*(\kappa_x,-\kappa_y)\end{aligned} \tag{3.2-5b}$$

Equations (3.2-5a) and (3.2-5b) imply the bi-spectral distribution functions $F_{jk}(\kappa_x,\kappa_y)$ and $F_{jk}(\kappa_x,-\kappa_y)$ are necessary for representing the covariance function $R_{jk}^{(1)}(\xi_x,\xi_y)$ of the real valued homogeneous stochastic fields $j^{(1)}(x,y)$ and $k^{(1)}(x,y)$ (see Fig. 3.2-1).

Equations (3.2-5a) and (3.2-5b) also imply that the two orthogonal increments $dZ_j(\kappa_x,\kappa_y)$ and $dZ_j(\kappa_x,-\kappa_y)$ are needed for the spectral representation of the real valued stochastic field $j^{(1)}(x,y)$ (see Fig. 3.2-1a). If $F_{jk}(\kappa_x,\kappa_y)=F_{jk}(\kappa_x,-\kappa_y)$ or $Z_j(\kappa_x,\kappa_y)=Z_j(\kappa_x,-\kappa_y)$, the stochastic field is called quadrant symmetry (see Fig. 3.2-1b))

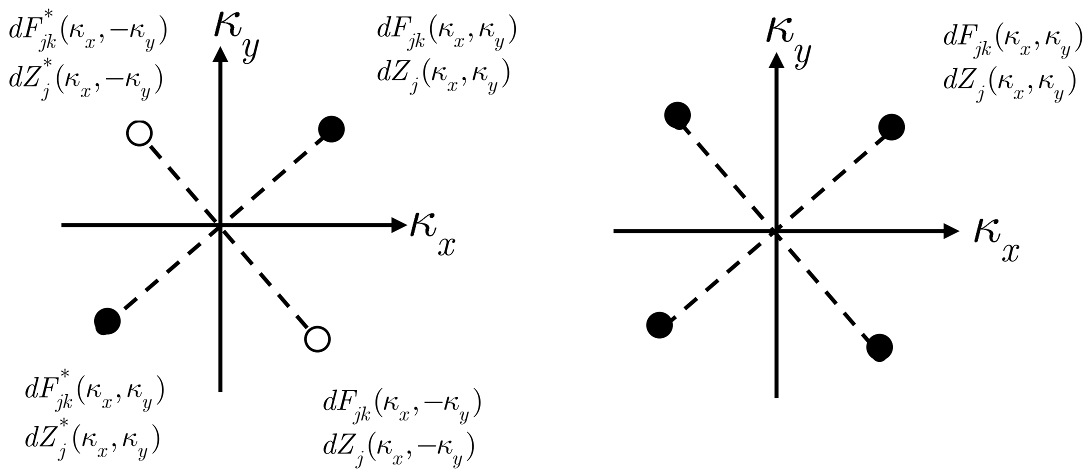

(a) Homogeneous Two-Dimensional Case (b) Quadrant Symmetry Case

Fig. 3.2-1 Characteristics of Homogenous Two-Dimensional Stochastic Fields in Wave Number Domain

Substitution of the conditions given by Eqs. (3.2-5a) and (3.2-5b) into Eqs. (3.1-6) and (3.1-7) or Eqs. (3.2-2) and (3.2-3) yields the required fundamental expressions for real valued two-dimensional stochastic fields such that

$$R_{jk}(\xi_x,\xi_y)=\int_0^\infty\int_0^\infty\begin{pmatrix}\cos(\kappa_x\xi_x+\kappa_y\xi_y)dF_{jk}^{(1)}(\kappa_x,\kappa_y)+\\ \sin(\kappa_x\xi_x+\kappa_y\xi_y)dF_{jk}^{(2)}(\kappa_x,\kappa_y)\end{pmatrix}$$

$$+\int_0^\infty\int_0^\infty\begin{pmatrix}\cos(\kappa_x\xi_x-\kappa_y\xi_y)dF_{jk}^{(1)}(\kappa_x,-\kappa_y)+\\ \sin(\kappa_x\xi_x-\kappa_y\xi_y)dF_{jk}^{(2)}(\kappa_x,-\kappa_y)\end{pmatrix} \tag{3.2-6a}$$

where $j=f,g$ and the field itself is

$$j(x,y)=\int_0^\infty\int_0^\infty\begin{pmatrix}\cos(\kappa_x x+\kappa_y y)dU_j^{(1)}(\kappa_x,\kappa_y)+\\ \sin(\kappa_x x+\kappa_y y)dU_j^{(2)}(\kappa_x,\kappa_y)\end{pmatrix}$$

$$+\int_0^\infty\int_0^\infty\begin{pmatrix}\cos(\kappa_x x-\kappa_y y)dU_j^{(1)}(\kappa_x,-\kappa_y)+\\ \sin(\kappa_x x-\kappa_y y)dU_j^{(2)}(\kappa_x,-\kappa_y)\end{pmatrix} \tag{3.2-6b}$$

It is easy to show that the real valued increments $dF_{jk}^{(1)},dF_{jk}^{(2)}$ and $dU_j^{(1)}$, $dU_j^{(2)}$ have the following requirements, by substituting Eq. (3.2-1) into Eqs. (2.2-2a), (2.2-2b) and (2.2-2c) for the conditions of the complex orthogonal increments.

$$E[dU_j^{(1)}(\kappa_x,\kappa_y)]=E[dU_j^{(2)}(\kappa_x,\kappa_y)]=0$$

$$E[dU_j^{(1)}(\kappa_x,\kappa_y)dU_k^{(1)}(\kappa'_x,\kappa'_y)]=E[dU_j^{(2)}(\kappa_x,\kappa_y)dU_k^{(2)}(\kappa'_x,\kappa')]$$

$$=\delta(\kappa_x-\kappa'_x)\delta(\kappa_y-\kappa'_y)dF_{jk}^{(1)}(\kappa'_x,\kappa'_y) \tag{3.2-7}$$

$$E[dU_j^{(2)}(\kappa_x,\kappa_y)dU_k^{(1)}(\kappa'_x,\kappa'_y)]=-E[dU_j^{(1)}(\kappa_x,\kappa_y)dU_k^{(2)}(\kappa'_x,\kappa'_y)]$$

$$=\begin{cases}\delta(\kappa_x-\kappa'_x)\delta(\kappa_y-\kappa'_y)dF_{jk}^{(2)}(\kappa'_x,\kappa') & j\neq k\\ 0 & j=k\end{cases}$$

It is also easy to show Eq. (3.2-6a), by using the spectral representation of the real valued field $j(x,y)$ given by Eq. (3.2-6b) and the orthogonal conditions for the real valued increments $dU_j^{(1)}$ and $dU_j^{(2)}$ given by Eq. (3.2-7). In fact,

$$
\begin{aligned}
R_{jk}^{(1)}(\xi_x,\xi_y) &= E[j^{(1)}(x+\xi_x, y+\xi_y)k^{(1)}(x,y)] \\
&= \int_0^\infty\int_0^\infty\int_0^\infty\int_0^\infty
\begin{pmatrix}
\cos(\kappa_x(x+\xi_x)+\kappa_y(y+\xi_y))dU_j^{(1)}(\kappa_x,\kappa_y)+ \\
\sin(\kappa_x(x+\xi_x)+\kappa_y(y+\xi_y))dU_j^{(2)}(\kappa_x,\kappa_y)+ \\
\cos(\kappa_x(x+\xi_x)-\kappa_y(y+\xi_y))dU_j^{(1)}(\kappa_x,-\kappa_y)+ \\
\sin(\kappa_x(x+\xi_x)-\kappa_y(y+\xi_y))dU_j^{(2)}(\kappa_x,-\kappa_y)
\end{pmatrix}\times \\
&\qquad\qquad
\begin{pmatrix}
\cos(\kappa_x'(x+\xi_x)+\kappa_y'(y+\xi_y))dU_j^{(1)}(\kappa_x',\kappa_y')+ \\
\sin(\kappa_x'(x+\xi_x)+\kappa_y'(y+\xi_y))dU_j^{(2)}(\kappa_x',\kappa_y')+ \\
\cos(\kappa_x'(x+\xi_x)-\kappa_y'(y+\xi_y))dU_j^{(1)}(\kappa_x',-\kappa_y')+ \\
\sin(\kappa_x'(x+\xi_x)-\kappa_y'(y+\xi_y))dU_j^{(2)}(\kappa_x',-\kappa_y')
\end{pmatrix} \\
&= \int_0^\infty\int_0^\infty
\begin{pmatrix}
\cos(\kappa_x\xi_x+\kappa_y\xi_y)dF_{jk}^{(1)}(\kappa_x,\kappa_y)+ \\
\sin(\kappa_x\xi_x+\kappa_y\xi_y)dF_{jk}^{(2)}(\kappa_x,\kappa_y)
\end{pmatrix} \\
&\quad + \int_0^\infty\int_0^\infty
\begin{pmatrix}
\cos(\kappa_x\xi_x-\kappa_y\xi_y)dF_{jk}^{(1)}(\kappa_x,-\kappa_y)+ \\
\sin(\kappa_x\xi_x-\kappa_y\xi_y)dF_{jk}^{(2)}(\kappa_x,-\kappa_y)
\end{pmatrix}
\end{aligned}
\qquad (3.2\text{-}8)
$$

4. SIMULATION METHOD

Consider the simulation problem of the homogeneous stochastic fields and under the condition that the power spectral density function matrix is specified such that

$$\boldsymbol{S}(\kappa) = \begin{pmatrix} S_{ff}(\kappa_x,\kappa_y) & S_{fg}(\kappa_x,\kappa_y) \\ S_{gf}(\kappa_x,\kappa_y) & S_{gg}(\kappa_x,\kappa_y) \end{pmatrix}, \quad S_{gf}(\kappa_x,\kappa_y) = S_{fg}^{*}(\kappa_x,\kappa_y) \tag{4.1}$$

Since the power spectral density function matrix constitutes the Hermitian and non-negative definite matrix, Eq. (4-1) can be decomposed as

$$\begin{pmatrix} a_{11} & 0 \\ a_{21} & a_{22} \end{pmatrix} \begin{pmatrix} a_{11}^{*} & a_{21}^{*} \\ 0 & a_{22}^{*} \end{pmatrix} = \begin{pmatrix} |\, a_{11} \,|^2 & a_{11}a_{21}^{*} \\ a_{21}a_{11}^{*} & |\, a_{21} \,|^2 + |\, a_{22} \,|^2 \end{pmatrix} \tag{4-2}$$

Where each element a_{jk} can be obtained as

$$a_{11} = |\, a_{11} \,|\, \mathrm{e}^{i\psi_1(\kappa_x,\kappa_y)} = \sqrt{S_{ff}(\kappa_x,\kappa_y)}\, \mathrm{e}^{i\psi_1(\kappa_x,\kappa_y)}$$

$$\begin{aligned} a_{21} &= |\, a_{21} \,|\, \mathrm{e}^{i\alpha_{21}(\kappa_x,\kappa_y)} \\ &= \frac{|\, S_{fg}(\kappa_x,\kappa_y) \,|}{\sqrt{S_{ff}(\kappa_x,\kappa_y)}}\, \mathrm{e}^{i(\psi_1(\kappa_x,\kappa_y)+\alpha_{21}(\kappa_x,\kappa_y))} \end{aligned} \tag{4-3a}$$

$$\begin{aligned} a_{22} &= |\, a_{22} \,|\, \mathrm{e}^{i\psi_2(\kappa_x,\kappa_y)} \\ &= \sqrt{\frac{S_{ff}(\kappa_x,\kappa_y)S_{gg}(\kappa_x,\kappa_y) - |\, S_{fg}(\kappa_x,\kappa_y) \,|^2}{S_{ff}(\kappa_x,\kappa_y)}}\, \mathrm{e}^{i\psi_2(\kappa_x,\kappa_y)} \end{aligned}$$

where $\psi_1(\kappa_x,\kappa_y)$ and $\psi_2(\kappa_x,\kappa_y)$ are arbitrary phase angles and

$$\alpha_{21}(\kappa_x,\kappa_y) = \tan^{-1}\left(\frac{\mathrm{Im}(S_{fg}(\kappa_x,\kappa_y))}{\mathrm{Re}(S_{fg}(\kappa_x,\kappa_y))} \right) \tag{4-3b}$$

On the other hand, the covariance of the orthogonal increment $dZ_j(\kappa_x, \kappa_y)$ is given by Eq. (3.1-8b) or Eq. (3.1-11a), that is

$$\begin{aligned} E[dZ_f(\kappa_x,\kappa_y)dZ_f^*(\kappa_x,\kappa_y)] &= S_{ff}(\kappa_x,\kappa_y)d\kappa_x d\kappa_y \\ E[dZ_f(\kappa_x,\kappa_y)dZ_g^*(\kappa_x,\kappa_y)] &= S_{fg}(\kappa_x,\kappa_y)d\kappa_x d\kappa_y \\ E[dZ_g(\kappa_x,\kappa_y)dZ_g^*(\kappa_x,\kappa_y)] &= S_{gg}(\kappa_x,\kappa_y)d\kappa_x d\kappa_y \end{aligned} \tag{4-4}$$

Comparison of Eqs. (4-2) and (4-4) motivates the introduction of a new definition for the orthogonal increments dZ_f and dZ_g to efficiently express the orthogonal increments in terms of the power spectral density functions as follows:

$$\begin{aligned} dZ_f &= dZ_{ff} \\ dZ_g &= dZ_{gf} + dZ_{gg} \end{aligned} \tag{4-5a}$$

where

$$E[dZ_{ff}dZ_{gg}^*] = E[dZ_{gf}dZ_{gg}^*] = 0 \tag{4-5b}$$

and similarly

$$\begin{aligned} dZ_f &= \frac{1}{2}(dU_{ff}^{(1)} - idU_{ff}^{(2)}) \\ dZ_g &= \frac{1}{2}(dU_{gf}^{(1)} - idU_{gf}^{(2)}) + \frac{1}{2}(dU_{gg}^{(1)} - idU_{gg}^{(2)}) \end{aligned} \tag{4-5c}$$

where $dU_{jk}^{(1)}$ and $dU_{jk}^{(2)}$ are real valued.

Substitution of Eq. (4-5a) into Eq. (4-4) and taking into account Eq. (4-5b) yields the following equation as

$$\begin{pmatrix} E[dZ_f dZ_f^*] & E[dZ_f dZ_g^*] \\ E[dZ_g dZ_f^*] & E[dZ_g dZ_g^*] \end{pmatrix} = \begin{pmatrix} E[| dZ_{ff} |^2] & E[dZ_{ff}dZ_{gf}^*] \\ E[dZ_{gf}dZ_{ff}^*] & E[| dZ_{gf} |^2 + | dZ_{gg} |^2] \end{pmatrix} \tag{4-6}$$

By comparison of Eq. (4-2) and Eq. (4-6), the orthogonal increments can be expressed in terms of a_{jk} which in turn is a function of the power spectral density function such that

$$\begin{aligned} dZ_{ff}(\kappa_x,\kappa_y) &= \mid a_{11} \mid \sqrt{d\kappa_x d\kappa_y}\ \mathrm{e}^{i\psi_1(\kappa_x,\kappa_y)} \\ dZ_{gf}(\kappa_x,\kappa_y) &= \mid a_{21} \mid \sqrt{d\kappa_x d\kappa_y}\ \mathrm{e}^{i(\psi_1(\kappa_x,\kappa_y)+\alpha_{21}(\kappa_x,\kappa_y))} \\ dZ_{gf}(\kappa_x,\kappa_y) &= \mid a_{22} \mid \sqrt{d\kappa_x d\kappa_y}\ \mathrm{e}^{i\psi_2(\kappa_x,\kappa_y)} \end{aligned} \tag{4-7}$$

Also, taking into account Eq. (4-5c),

$$\begin{aligned} dU_{ff}^{(1)}(\kappa_x,\kappa_y) &= 2 \mid a_{11} \mid \sqrt{d\kappa_x d\kappa_y}\cos\psi_1(\kappa_x,\kappa_y) \\ dU_{ff}^{(2)}(\kappa_x,\kappa_y) &= -2 \mid a_{11} \mid \sqrt{d\kappa_x d\kappa_y}\sin\psi_1(\kappa_x,\kappa_y) \\ \\ dU_{gf}^{(1)}(\kappa_x,\kappa_y) &= 2 \mid a_{21} \mid \sqrt{d\kappa_x d\kappa_y}\cos(\psi_1(\kappa_x,\kappa_y)+\alpha_{21}(\kappa_x,\kappa_y)) \\ dU_{gf}^{(2)}(\kappa_x,\kappa_y) &= -2 \mid a_{21} \mid \sqrt{d\kappa_x d\kappa_y}\sin(\psi_1(\kappa_x,\kappa_y)+\alpha_{21}(\kappa_x,\kappa_y)) \\ \\ dU_{gg}^{(1)}(\kappa_x,\kappa_y) &= 2 \mid a_{22} \mid \sqrt{d\kappa_x d\kappa_y}\cos\psi_2(\kappa_x,\kappa_y) \\ dU_{gg}^{(2)}(\kappa_x,\kappa_y) &= -2 \mid a_{22} \mid \sqrt{d\kappa_x d\kappa_y}\sin\psi_2(\kappa_x,\kappa_y) \end{aligned} \tag{4-8}$$

If we choose independent random phases uniformly distributed between 0 and 2π for $\psi_1(\kappa_x,\kappa_y)$ and $\psi_2(\kappa_x,\kappa_y)$, it is easy to show that Eqs. (4-7) and (4-8) satisfy Eqs. (3.1-11a) or (3.2-7), respectively.

From Eqs. (3.2-6b) and (2.3-8), the real valued stochastic fields $f^{(1)}(x,y)$ and $g^{(1)}(x,y)$ can be expressed as

$$\begin{aligned} f^{(1)}(x,y) = & \int_0^\infty\int_0^\infty 2 \mid a_{11}(\kappa_x,\kappa_y) \mid \sqrt{d\kappa_x d\kappa_y}\cos A_{11}(\kappa_x,\kappa_y) \\ & + \int_0^\infty\int_0^\infty 2 \mid a_{11}(\kappa_x,-\kappa_y) \mid \sqrt{d\kappa_x d\kappa_y}\cos A_{11}(\kappa_x,-\kappa_y) \end{aligned} \tag{4-9a}$$

$$\begin{aligned} A_{11}(\kappa_x,\kappa_y) &= (\kappa_x x + \kappa_y y + \psi_1(\kappa_x,\kappa_y)) \\ A_{11}(\kappa_x,-\kappa_y) &= (\kappa_x x - \kappa_y y + \psi_1(\kappa_x,-\kappa_y)) \end{aligned}$$

and

$$
\begin{aligned}
g^{(1)}(x,y) = &\int_0^\infty\int_0^\infty 2\mid a_{21}(\kappa_x,\kappa_y)\mid\sqrt{d\kappa_x d\kappa_y}\cos A_{21}(\kappa_x,\kappa_y)\\
&+\int_0^\infty\int_0^\infty 2\mid a_{21}(\kappa_x,-\kappa_y)\mid\sqrt{d\kappa_x d\kappa_y}\cos A_{21}(\kappa_x,-\kappa_y)\\
&+\int_0^\infty\int_0^\infty 2\mid a_{22}(\kappa_x,\kappa_y)\mid\sqrt{d\kappa_x d\kappa_y}\cos A_{22}(\kappa_x,\kappa_y)\\
&+\int_0^\infty\int_0^\infty 2\mid a_{22}(\kappa_x,-\kappa_y)\mid\sqrt{d\kappa_x d\kappa_y}\cos A_{22}(\kappa_x,-\kappa_y)
\end{aligned}
\tag{4-9b}
$$

$$
\begin{aligned}
A_{21}(\kappa_x,\kappa_y) &= (\kappa_x x+\kappa_y y+\psi_1(\kappa_x,\kappa_y)+\alpha_{21}(\kappa_x,\kappa_y))\\
A_{21}(\kappa_x,-\kappa_y) &= (\kappa_x x-\kappa_y y+\psi_1(\kappa_x,-\kappa_y)+\alpha_{21}(\kappa_x,-\kappa_y))\\
A_{22}(\kappa_x,\kappa_y) &= (\kappa_x x+\kappa_y y+\psi_2(\kappa_x,\kappa_y))\\
A_{22}(\kappa_x,-\kappa_y) &= (\kappa_x x-\kappa_y y+\psi_2(\kappa_x,-\kappa_y))
\end{aligned}
$$

The integrals mean, for $d\kappa_x \to 0, d\kappa_y \to 0$ and $\kappa_{xn} = nd\kappa_x, \kappa_{ym} = md\kappa_y$

$$
\begin{aligned}
f^{(1)}(x,y) = &\sum_{n=1}^{N}\sum_{m=1}^{M} 2\mid a_{11}(\kappa_{xn},\kappa_{ym})\mid\sqrt{d\kappa_x d\kappa_y}\cos A_{11}(\kappa_{xn},\kappa_{ym})\\
&+2\mid a_{11}(\kappa_{xn},-\kappa_{ym})\mid\sqrt{d\kappa_x d\kappa_y}\cos A_{11}(\kappa_{xn},-\kappa_{ym})
\end{aligned}
\tag{4-10a}
$$

$$
\begin{aligned}
A_{11}(\kappa_{xn},\kappa_{ym}) &= (\kappa_{xn}x+\kappa_{ym}y+\psi_1(\kappa_{xn},\kappa_{ym}))\\
A_{11}(\kappa_{xn},-\kappa_{ym}) &= (\kappa_{xn}x-\kappa_{ym}y+\psi_1(\kappa_{xn},-\kappa_{ym}))
\end{aligned}
$$

It is noted here that the uniformly distributed random angles $\psi_1(\kappa_{xn},\kappa_{ym})$ and $\psi_1(\kappa_{xn},-\kappa_{ym})$ between 0 and 2π are independent each other.

and

$$
\begin{aligned}
g^{(1)}(x,y) = \sum_{n=1}^{N}\sum_{m=1}^{M} & 2 \mid a_{21}(\kappa_{xn},\kappa_{ym}) \mid \sqrt{d\kappa_x d\kappa_y} \cos A_{21}(\kappa_{xn},\kappa_{ym}) \\
& + 2 \mid a_{21}(\kappa_{xn},-\kappa_{ym}) \mid \sqrt{d\kappa_x d\kappa_y} \cos A_{21}(\kappa_{xn},-\kappa_{ym}) \\
& + 2 \mid a_{22}(\kappa_{xn},\kappa_{ym}) \mid \sqrt{d\kappa_x d\kappa_y} \cos A_{22}(\kappa_{xn},\kappa_{ym}) \\
& + 2 \mid a_{22}(\kappa_{xn},-\kappa_{ym}) \mid \sqrt{d\kappa_x d\kappa_y} \cos A_{22}(\kappa_{xn},-\kappa_{ym})
\end{aligned}
\tag{4-10b}
$$

$$
\begin{aligned}
A_{21}(\kappa_{xn},\kappa_{ym}) &= (\kappa_{xn}x + \kappa_{ym}y + \psi_1(\kappa_{xn},\kappa_{ym}) + \alpha_{21}(\kappa_{xn},\kappa_{ym})) \\
A_{21}(\kappa_{xn},-\kappa_{ym}) &= (\kappa_{xn}x - \kappa_{ym}y + \psi_1(\kappa_{xn},-\kappa_{ym}) + \alpha_{21}(\kappa_{xn},-\kappa_{ym})) \\
A_{22}(\kappa_{xn},\kappa_{ym}) &= (\kappa_{xn}x + \kappa_{ym}y + \psi_2(\kappa_{xn},\kappa_{ym})) \\
A_{22}(\kappa_{xn},-\kappa_{ym}) &= (\kappa_{xn}x - \kappa_{ym}y + \psi_2(\kappa_{xn},-\kappa_{ym}))
\end{aligned}
$$

where the uniformly distributed random angles $\psi_1(\kappa_{xn},\kappa_{ym})$, $\psi_1(\kappa_{xn},-\kappa_{ym})$, $\psi_2(\kappa_{xn},\kappa_{ym})$ and $\psi_2(\kappa_{xn},-\kappa_{ym})$ are also independent each other. And

$$
\begin{aligned}
& \mid a_{11}(\kappa_{xn},\kappa_{ym}) \mid = \sqrt{S_{ff}(\kappa_{xn},\kappa_{ym})} \\
& \mid a_{21}(\kappa_{xn},\kappa_{ym}) \mid = \frac{\mid S_{fg}(\kappa_{xn},\kappa_{ym}) \mid}{\sqrt{S_{ff}(\kappa_{xn},\kappa_{ym})}} \\
& \mid a_{22}(\kappa_{xn},\kappa_{ym}) \mid = \sqrt{\frac{S_{ff}(\kappa_{xn},\kappa_{ym})S_{gg}(\kappa_{xn},\kappa_{ym}) - \mid S_{fg}(\kappa_{xn},\kappa_{ym}) \mid^2}{S_{ff}(\kappa_{xn},\kappa_{ym})}}
\end{aligned}
\tag{4-10c}
$$

and

$$
\alpha_{21}(\kappa_{xn},\kappa_{ym}) = \tan^{-1}\left(\frac{\mathrm{Im}(S_{fg}(\kappa_{xn},\kappa_{ym}))}{\mathrm{Re}(S_{fg}(\kappa_{xn},\kappa_{ym}))}\right) \tag{4-10d}
$$

If the fields and are quadrant symmetry where the power spectral density function satisfies $S_{jk}(\kappa_x,\kappa_y) = S_{jk}(\kappa_x,-\kappa_y)$ (see Fig. 3.2-1), then

$$
\begin{aligned}
& a_{jk}(\kappa_{xn},\kappa_{ym}) = a_{jk}(\kappa_{xn},-\kappa_{ym}), \quad j,k = 1,2 \\
& \alpha_{21}(\kappa_{xn},\kappa_{ym}) = \alpha_{21}(\kappa_{xn},-\kappa_{ym})
\end{aligned}
\tag{4-11}
$$

Hence, Eq. (2.3-10) reduce to, for quadrant symmetry,

$$f^{(1)}(x,y)=\sum_{n=1}^{N}\sum_{m=1}^{M}2\,|\,a_{11}(\kappa_{xn},\kappa_{ym})\,|\,\sqrt{d\kappa_x d\kappa_y}\begin{pmatrix}\cos A_{11}(\kappa_{xn},\kappa_{ym})+\\ \cos A_{11}(\kappa_{xn},-\kappa_{ym})\end{pmatrix} \quad (4\text{-}12a)$$

and

$$\begin{aligned}g^{(1)}(x,y)=\sum_{n=1}^{N}\sum_{m=1}^{M}&2\,|\,a_{21}(\kappa_{xn},\kappa_{ym})\,|\,\sqrt{d\kappa_x d\kappa_y}\begin{pmatrix}\cos A_{21}(\kappa_{xn},\kappa_{ym})+\\ \cos A_{21}(\kappa_{xn},-\kappa_{ym})\end{pmatrix}\\ &+2\,|\,a_{22}(\kappa_{xn},\kappa_{ym})\,|\,\sqrt{d\kappa_x d\kappa_y}\begin{pmatrix}\cos A_{22}(\kappa_{xn},\kappa_{ym})+\\ \cos A_{22}(\kappa_{xn},-\kappa_{ym})\end{pmatrix}\end{aligned} \quad (4\text{-}12b)$$

The above Eqs. (4.10) and (4.12) are suitable for the computer simulation of real valued $f^{(1)}(x,y)$ and $g^{(1)}(x,y)$.

The wave number vector is assumed to be located in the first (1st) quadrant so that all the wave numbers are positive (negative). Then Eqs. (4.10) and (4.12) reduce to as follows, although their simulated stochastic fields satisfy the target power spectral density (or correlation) functions.

$$f^{(1)}(x,y)=\sum_{n=1}^{N}\sum_{m=1}^{M}2\,|\,a_{11}(\kappa_{xn},\kappa_{ym})\,|\,\sqrt{d\kappa_x d\kappa_y}\cos A_{11}(\kappa_{xn},\kappa_{ym}) \quad (4\text{-}13a)$$

and

$$\begin{aligned}g^{(1)}(x,y)=\sum_{n=1}^{N}\sum_{m=1}^{M}&2\,|\,a_{21}(\kappa_{xn},\kappa_{ym})\,|\,\sqrt{d\kappa_x d\kappa_y}\cos A_{21}(\kappa_{xn},\kappa_{ym})\\ &+2\,|\,a_{22}(\kappa_{xn},\kappa_{ym})\,|\,\sqrt{d\kappa_x d\kappa_y}\cos A_{22}(\kappa_{xn},\kappa_{ym})\end{aligned} \quad (4\text{-}13b)$$

The above simulated fields may be called as the first quadrant symmetry. Eq. (4-13) was proposed by Shinozuka and Jan (1972).

Figure 4.1 shows schematically the wave number field of the Bi-directional wave number (quadrant symmetry) where both $A_{jk}(\kappa_{xn},\kappa_{ym})$ and

$A_{jk1}(\kappa_{xn}, -\kappa_{ym})$ are taken into account as Eq. (4.12). If the field is the first quadrant symmetry, Uni-directional wave number where only $A_{jk}(\kappa_{xn}, \kappa_{ym})$ is taken into account such as Eq. (4.13). Therefore, the first quadrant symmetry field shows a random field with directional characteristics, while the directional nature cannot be seen for the quadrant symmetry field (Chapter 6).

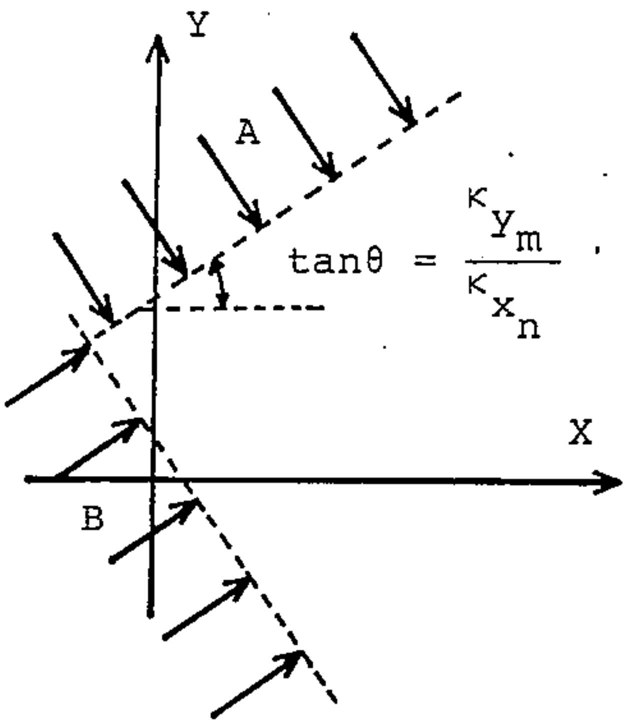

Fig. 4.1 Bi-Directional Wave Number in X-Y Plane

5. TIME-SPACE STOCHASTIC FIELDS

In the previous Chapters we were concerned with stochastic fields whose sample functions are continuous functions of the space coordinates x and y. We now turn to a more general case where the stochastic fields are functions of time as well as the space coordinates. This Chapter presents the relationships of the various second moments of the complex valued time space fields, and also only the results of the spectral representation of the real valued time space fields, because the real valued time space stochastic fields are obvious from the procedure shown in Chapter 4.

5.1 Second Moments of Time-Space Stochastic Fields

As defined in Chapters 2 and 3, the complex valued time space stochastic fields $f(x,y,t)$ and $g(x,y,t)$ can be defined as

$$\begin{aligned} f(x,y,t) &= f^{(1)}(x,y,t) + if^{(2)}(x,y,t) \\ g(x,y,t) &= g^{(1)}(x,y,t) + ig^{(2)}(x,y,t) \end{aligned} \tag{5.1-1}$$

where $f^{(1)}, f^{(2)}, g^{(1)}$ and $g^{(2)}$ are the real valued stochastic fields. The mean can be defined as

$$\begin{aligned} E[f(x,y,t)] &= E[f^{(1)}(x,y,t)] + iE[f^{(2)}(x,y,t)] \\ E[g(x,y,t)] &= E[g^{(1)}(x,y,t)] + iE[g^{(2)}(x,y,t)] \end{aligned} \tag{5.1-2}$$

where $E[\bullet]$ is the expectation operator.

Now suppose that the fields are stationary, homogeneous and zero mean.

Then, the time space covariance function of the fields can be written in matrix form as

$$\boldsymbol{R}(\xi_x,\xi_y,\tau)=\begin{pmatrix} R_{ff}(\xi_x,\xi_y,\tau) & R_{fg}(\xi_x,\xi_y,\tau) \\ R_{gf}(\xi_x,\xi_y,\tau) & R_{gg}(\xi_x,\xi_y,\tau) \end{pmatrix}$$

$$=\begin{pmatrix} E[f(x+\xi_x,y+\xi_y,t+\tau)f^*(x,y,t)] & E[f(x+\xi_x,y+\xi_y,t+\tau)g^*(x,y,t)] \\ E[g(x+\xi_x,y+\xi_y,t+\tau)f^*(x,y,t)] & E[g(x+\xi_x,y+\xi_y,t+\tau)g^*(x,y,t)] \end{pmatrix}$$

(5.1-3)

From the definition given by Eq. (5.1-3), the time space covariance function possesses the property such that

$$R_{jk}(\xi_x,\xi_y,\tau)=R^*_{kj}(-\xi_x,-\xi_y,-\tau),\quad j,k=f,g \tag{5.1-4}$$

That is, the covariance matrix is Hermitian.

Transforming the time lag τ into the frequency ω by means of the Wiener Kintchine transform yields the temporal frequency spatial spectral density function as a function of separation distances ξ_x and ξ_y:

$$B_{jk}(\xi_x,\xi_y,\omega)=\frac{1}{2\pi}\int_{-\infty}^{\infty}\mathrm{e}^{i\omega\tau}R_{kj}(\xi_x,\xi_y,\tau)d\tau \tag{5.1-5a}$$

By performing an inverse transformation, we can reclaim $R_{jk}(\xi_x,\xi_y,\tau)$ as

$$R_{kj}(\xi_x,\xi_y,\tau)=\int_{-\infty}^{\infty}\mathrm{e}^{-i\omega\tau}B_{jk}(\xi_x,\xi_y,\omega)d\omega \tag{5.1-5b}$$

If the separation distances ξ_x and ξ_y are zero, the temporal frequency spatial spectral density function is expressed as (at any point x and y):

$$B_{jk}(0,0,\omega)=S_{jk}(\omega) \tag{5.1-6}$$

Normalization of the temporal frequency cross spectral density function with respect to its value at the zero separation distances gives the frequency dependent spatial covariance function as follows:

$$\gamma_{jk}(\xi_x, \xi_y, \omega) = \frac{B_{jk}(\xi_x, \xi_y, \omega)}{S_{jk}(\omega)} \tag{5.1-7}$$

The spatial covariance function can be defined as

$$B_{jk}(\xi_x, \xi_y) = R_{jk}(\xi_x, \xi_y, \tau = 0) \tag{5.1-8a}$$

and hence, with the aid of Eqs. (5.1-5a) and (5.1-7),

$$B_{jk}(\xi_x, \xi_y) = \int_{-\infty}^{\infty} B_{jk}(\xi_x, \xi_y, \omega) d\omega = \int_{-\infty}^{\infty} S_{jk}(\omega) \gamma_{jk}(\xi_x, \xi_y, \omega) d\omega \tag{5.1-8b}$$

Thus, the spatial covariance function is a weighted integral of the frequency dependent spatial covariance function $\gamma_{jk}(\xi_x, \xi_y, \omega)$ with the point cross spectral density function $S_{jk}(\omega)$ as the weight.

If the time space stochastic fields are assumed to be ergodic, the spatial covariance function may be estimated from the temporal average such that

$$\begin{aligned} B_{jk}(\xi_x, \xi_y) &= R_{jk}(\xi_x, \xi_y, \tau = 0) \\ &= \lim_{T \to \infty} \frac{1}{T} \int_0^T j_n(x + \xi_x, y + \xi_y, t) k_n^*(x, y, t) dt \end{aligned} \tag{5.1-9b}$$

or from the following spatial average

$$\begin{aligned} B_{jk}(\xi_x, \xi_y) &= R_{jk}(\xi_x, \xi_y, \tau = 0) \\ &= \lim_{\substack{L_x \to \infty \\ L_y \to \infty}} \frac{1}{L_x L_y} \int_0^{L_x} \int_0^{L_y} j_n(x + \xi_x, y + \xi_y, t) k_n^*(x, y, t) dx dy \end{aligned} \tag{5.1-9b}$$

in which $j_n(x, y, t)$ represents the n-th sample function of real valued

$j(x,y,t)$, where $j = f,g$. However, in practice, Eq. (5.1-9b) cannot usually be used since the observations $j_n(x,y,t)$ are made at only a few discrete locations along the x and y axes and therefore the integration of Eq. (5.1-9b) is not possible.

Similarly, transforming the separation distances ξ_x and ξ_y into the wave numbers κ_x and κ_y by means of the Wiener Khintchine transform gives the temporal covariance spatial cross wave number spectral density function $C_{jk}(\kappa_x,\kappa_y,\tau)$ as a function of τ:

$$C_{jk}(\kappa_x,\kappa_y,\tau) = \frac{1}{(2\pi)^2}\int_{-\infty}^{\infty}\int_{-\infty}^{\infty} \mathrm{e}^{-i(\kappa_x\xi_x+\kappa_y\xi_y)} R_{jk}(\xi_x,\xi_y,\tau)d\xi_x d\xi_y \qquad (5.1\text{-}10a)$$

By performing an inverse transformation, we can reclaim $R_{jk}(\xi_x,\xi_y,\tau)$ as

$$R_{jk}(\xi_x,\xi_y,\tau) = \int_{-\infty}^{\infty}\int_{-\infty}^{\infty} \mathrm{e}^{i(\kappa_x\xi_x+\kappa_y\xi_y)} C_{jk}(\kappa_x,\kappa_y,\tau)d\kappa_x d\kappa_y \qquad (5.1\text{-}10b)$$

Finally, transforming both the time lag and the separation distances into the frequency and wave numbers by means of the Wiener Khintchine transform gives the frequency wave number cross spectral density function such that

$$S_{jk}(\kappa_x,\kappa_y,\omega) = \frac{1}{(2\pi)^3}\int_{-\infty}^{\infty}\int_{-\infty}^{\infty}\int_{-\infty}^{\infty} \mathrm{e}^{-i(\kappa_x\xi_x+\kappa_y\xi_y-\omega\tau)} R_{jk}(\xi_x,\xi_y,\tau)d\xi_x d\xi_y d\tau \qquad (5.1\text{-}11a)$$

From the inverse transformation

$$R_{jk}(\xi_x,\xi_y,\tau) = \int_{-\infty}^{\infty}\int_{-\infty}^{\infty}\int_{-\infty}^{\infty} \mathrm{e}^{i(\kappa_x\xi_x+\kappa_y\xi_y-\omega\tau)} S_{jk}(\kappa_x,\kappa_y,\omega)d\kappa_x d\kappa_y d\omega \qquad (5.1\text{-}11b)$$

Due to Eqs. (5.1-5a), (5.1-5b) and (5.1-10a), the frequency wave number spectral density function $S_{jk}(\kappa_x,\kappa_y,\omega)$ is also related to $B_{jk}(\xi_x,\xi_y,\omega)$ and $C_{jk}(\kappa_x,\kappa_y,\tau)$ such that

$$S_{jk}(\kappa_x,\kappa_y,\omega)=\frac{1}{(2\pi)^2}\int_{-\infty}^{\infty}\int_{-\infty}^{\infty}\mathrm{e}^{-i(\kappa_x\xi_x+\kappa_y\xi_y)}B_{jk}(\xi_x,\xi_y,\omega)d\xi_x d\xi_y \tag{5.1-12a}$$

and

$$S_{jk}(\kappa_x,\kappa_y,\omega)=\frac{1}{2\pi}\int_{-\infty}^{\infty}\mathrm{e}^{-i\omega\tau}C_{jk}(\kappa_x,\kappa_y,\tau)d\tau \tag{5.1-13a}$$

By the inverse transformation

$$B_{jk}(\xi_x,\xi_y,\omega)=\int_{-\infty}^{\infty}\int_{-\infty}^{\infty}\mathrm{e}^{i(\kappa_x\xi_x+\kappa_y\xi_y)}S_{jk}(\kappa_x,\kappa_y,\omega)d\kappa_x d\kappa_y \tag{5.1-12b}$$

and

$$C_{jk}(\kappa_x,\kappa_y,\tau)=\int_{-\infty}^{\infty}\mathrm{e}^{i\omega\tau}S_{jk}(\kappa_x,\kappa_y,\omega)d\omega \tag{5.1-13b}$$

And the point spectral density function defined by Eq. (5.1-6) is also written as

$$S_{jk}(\omega)=B_{jk}(0,0,\omega)=\int_{-\infty}^{\infty}\int_{-\infty}^{\infty}S_{jk}(\kappa_x,\kappa_y,\omega)d\kappa_x d\kappa_y \tag{5.1-14}$$

Similar to Eq. (5.1-7), normalization of the frequency wave number spectral density function $S_{jk}(\kappa_x,\kappa_y,\omega)$ with respect to the point spectral density function $S_{jk}(\omega)$ yields the frequency dependent wave number spectral density function as follows:

$$\tilde{\gamma}_{jk}(\kappa_x,\kappa_y,\omega)=\frac{S_{jk}(\kappa_x,\kappa_y,\omega)}{S_{jk}(\omega)} \tag{5.1-15}$$

The spatial wave number spectral density function $S_{jk}(\kappa_x,\kappa_y)$ can be defined as $S_{jk}(\kappa_x,\kappa_y)=C_{jk}(\kappa_x,\kappa_y,\tau=0)$ and hence, with the aid of Eqs. (5.1-13b) and (5.1-15),

$$\begin{aligned} S_{jk}(\kappa_x,\kappa_y) &= C_{jk}(\kappa_x,\kappa_y,\tau=0) \\ &= \int_{-\infty}^{\infty} S_{jk}(\kappa_x,\kappa_y,\omega)d\omega \\ &= \int_{-\infty}^{\infty} S_{jk}(\omega)\tilde{\gamma}_{jk}(\kappa_x,\kappa_y,\omega)d\omega \end{aligned} \tag{5.1-16}$$

As described above, there is a close relationship among the various functions which are summarized in Fig. 5.1-1. From a general characterization point of view, the frequency wave number spectral density function $S_{jk}(\kappa_x,\kappa_y,\omega)$ defined by Eq. (5.1-11a) may be more useful because this function plays a central role when we perform an analysis similar to that used for the spectral representation of stochastic fields as described in Chapter 2 and 3. On the other hand, the spatial covariance function $B_{jk}(\xi_x,\xi_y)$ and the spatial spectral density function $S_{jk}(\kappa_x,\kappa_y)$ are also important functions to characterize the spatial variation of the time space stochastic fields $j(x,y,t)$ and $k(x,y,t)$. In fact, the spatial variation of earthquake ground motion displacements is of major significance or the response of underground lifeline structures such as pipelines. In Chapter 6, a numerical example for the spatial variation of earthquake ground displacement is presented.

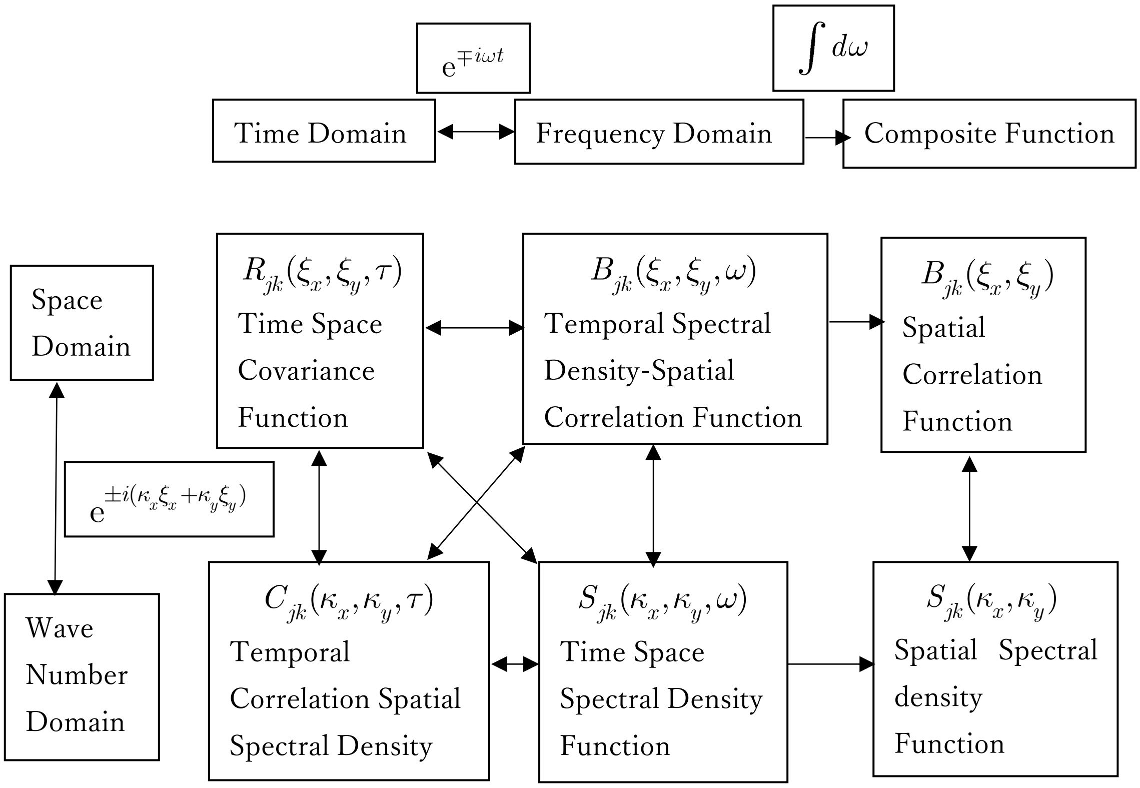

$$S_{jk}(\kappa_x,\kappa_y,\omega)=\frac{1}{(2\pi)^3}\int_{-\infty}^{\infty}\int_{-\infty}^{\infty}\int_{-\infty}^{\infty}\mathrm{e}^{-i(\kappa_x\xi_x+\kappa_y\xi_y-\omega\tau)}R_{jk}(\xi_x,\xi_y,\tau)d\xi_x d\xi_y d\tau$$

$$R_{jk}(\xi_x,\xi_y,\tau)=\int_{-\infty}^{\infty}\int_{-\infty}^{\infty}\int_{-\infty}^{\infty}\mathrm{e}^{i(\kappa_x\xi_x+\kappa_y\xi_y-\omega\tau)}S_{jk}(\kappa_x,\kappa_y,\omega)d\kappa_x d\kappa_y d\omega$$

Fig. 5.1-1 Relationship among the Various Second Moments for Stationary-Homogeneous Time-Space Stochastic Fields

5.2 Spectral Representation of Time Space Fields

Since the formulation is just same to the two-dimensional stochastic fields described in Chapters 3 and 4, we show only the results of the spectral representation of time space stochastic fields and their simulation method.

For the time space stochastic fields, we must take into account for the four combinations of frequency wave numbers as shown in Fig. 5.2-1, while two combinations are necessary for the two-dimensional stochastic fields.

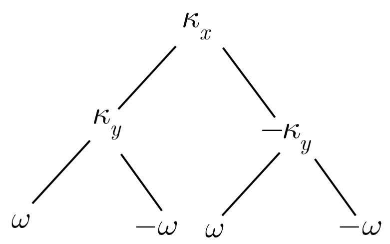

Fig. 5.2-1 Four Combinations of Frequency Wave Numbers for Time Space Stochastic Field

By considering the four combinations of frequency wave numbers in the real valued two-dimensional stochastic fields given by Eqs. (4-9a) and (4.9b), the spectral representation of time space stochastic fields is given such that

$$f^{(1)}(x,y,t)=\int_0^\infty\int_0^\infty\int_0^\infty 2\mid a_{11}(\kappa_x,\kappa_y,\omega)\mid\sqrt{d\kappa_x d\kappa_y d\omega}\cos A_{11}(\kappa_x,\kappa_y,\omega)$$
$$+\int_0^\infty\int_0^\infty 2\mid a_{11}(\kappa_x,\kappa_y,-\omega)\mid\sqrt{d\kappa_x d\kappa_y d\omega}\cos A_{11}(\kappa_x,\kappa_y,-\omega)$$
$$+\int_0^\infty\int_0^\infty 2\mid a_{11}(\kappa_x,-\kappa_y,\omega)\mid\sqrt{d\kappa_x d\kappa_y d\omega}\cos A_{11}(\kappa_x,-\kappa_y,\omega) \qquad (5.2\text{-}1)$$
$$+\int_0^\infty\int_0^\infty 2\mid a_{11}(\kappa_x,-\kappa_y,-\omega)\mid\sqrt{d\kappa_x d\kappa_y d\omega}\cos A_{11}(\kappa_x,-\kappa_y,-\omega)$$

$$A_{11}(\kappa_x,\kappa_y,\omega)=(\kappa_x x+\kappa_y y+\psi_1(\kappa_x,\kappa_y,\omega))$$

$$A_{11}(\kappa_x,-\kappa_y,\omega)=(\kappa_x x-\kappa_y y+\psi_1(\kappa_x,-\kappa_y,\omega))$$

In order to make above equation simple, we express it such as

$$f^{(1)}(x,y,t)=\int_0^\infty\int_0^\infty\int_0^\infty 2\sum_{I_y,I_\omega=\pm1}\begin{pmatrix}\mid a_{11}(\kappa_x,I_y\kappa_y,I_\omega\omega)\mid\sqrt{d\kappa_x d\kappa_y d\omega}\times\\ \cos A_{11}(I_y\kappa_y,I_\omega\omega)\end{pmatrix}$$
$$(5.2\text{-}2a)$$
$$A_{11}(\kappa_x,I_y\kappa_y,I_\omega\omega)=(\kappa_x x+I_y\kappa_y y+\psi_1(\kappa_x,I_y\kappa_y,I_\omega\omega))$$

and

$$g^{(1)}(x,y,t)=\int_0^\infty\int_0^\infty\int_0^\infty 2\sum_{I_y,I_\omega=\pm1}\begin{pmatrix}\mid a_{21}(\kappa_x,I_y\kappa_y,I_\omega\omega)\mid\sqrt{d\kappa_x d\kappa_y d\omega}\times\\ \cos A_{21}(\kappa_x,I_y\kappa_y,I_\omega\omega)\\ \mid a_{22}(\kappa_x,I_y\kappa_y,I_\omega\omega)\mid\sqrt{d\kappa_x d\kappa_y d\omega}\times\\ \cos A_{22}(\kappa_x,I_y\kappa_y,I_\omega\omega)\end{pmatrix}$$

$$A_{21}(\kappa_x,I_y\kappa_y,I_\omega\omega)=\begin{pmatrix}\kappa_x x+I_y\kappa_y y+\psi_1(\kappa_x,I_y\kappa_y,I_\omega\omega)+\\ \alpha_{21}(\kappa_x,I_y\kappa_y,I_\omega\omega)\end{pmatrix} \qquad (5.2\text{-}2b)$$

$$A_{22}(\kappa_x,I_y\kappa_y,I_\omega\omega)=(\kappa_x x+I_y\kappa_y y+\psi_2(\kappa_x,I_y\kappa_y,I_\omega\omega))$$

$$| a_{11}(\kappa_x, I_y\kappa_y, I_\omega\omega) |= \sqrt{S_{ff}(\kappa_x, I_y\kappa_y, I_\omega\omega)}$$

$$| a_{21}(\kappa_x, I_y\kappa_y, I_\omega\omega) |= \frac{| S_{fg}(\kappa_x, I_y\kappa_y, I_\omega\omega) |}{\sqrt{S_{ff}(\kappa_x, I_y\kappa_y, I_\omega\omega)}} \quad (5.2\text{-}2c)$$

$$| a_{22}(\kappa_x, I_y\kappa_y, I_\omega\omega) |= \sqrt{\frac{\begin{pmatrix} S_{ff}(\kappa_x, I_y\kappa_y, I_\omega\omega) S_{gg}(\kappa_x, I_y\kappa_y, I_\omega\omega) - \\ | S_{fg}(\kappa_x, I_y\kappa_y, I_\omega\omega) |^2 \end{pmatrix}}{S_{ff}(\kappa_x, I_y\kappa_y, I_\omega\omega)}}$$

and

$$\alpha_{21}(\kappa_x, I_y\kappa_y, I_\omega\omega) = \tan^{-1}\left(\frac{\mathrm{Im}(S_{fg}(\kappa_x, I_y\kappa_y, I_\omega\omega))}{\mathrm{Re}(S_{fg}(\kappa_x, I_y\kappa_y, I_\omega\omega))}\right) \quad (5.2\text{-}2d)$$

If the fields are quadrant symmetry, that is, the four spectral density function are same such as

$$| a_{11}(\kappa_x, I_y\kappa_y, I_\omega\omega) |=| a_{11}(\kappa_x, \kappa_y, \omega) |$$

$$| a_{21}(\kappa_x, I_y\kappa_y, I_\omega\omega) |=| a_{21}(\kappa_x, \kappa_y, \omega) | \quad (5.2\text{-}3)$$

$$| a_{22}(\kappa_x, I_y\kappa_y, I_\omega\omega) |=| a_{22}(\kappa_x, \kappa_y, \omega) |$$

Then, the spectral representation of real valued time space stochastic fields is given such that

$$f^{(1)}(x, y, t) = \int_0^\infty \int_0^\infty \int_0^\infty 2 \sum_{I_y, I_\omega = \pm 1} \begin{pmatrix} | a_{11}(\kappa_x, \kappa_y, \omega) | \sqrt{d\kappa_x d\kappa_y d\omega} \times \\ \cos A_{11}(\kappa_x, I_y\kappa_y, I_\omega\omega) \end{pmatrix}$$

$$A_{11}(\kappa_x, I_y\kappa_y, I_\omega\omega) = (\kappa_x x + I_y\kappa_y y + \psi_1(\kappa_x, I_y\kappa_y, I_\omega\omega)) \quad (5.2\text{-}2a)$$

and

$$g^{(1)}(x,y,t)=\int_0^\infty\int_0^\infty\int_0^\infty 2\sum_{I_y,I_\omega=\pm1}\begin{pmatrix}|\,a_{21}(\kappa_x,\kappa_y,\omega)\,|\sqrt{d\kappa_x d\kappa_y d\omega}\times\\ \cos A_{21}(\kappa_x,I_y\kappa_y,I_\omega\omega)+\\ \\ |\,a_{22}(\kappa_x,\kappa_y,\omega)\,|\sqrt{d\kappa_x d\kappa_y d\omega}\times\\ \cos A_{22}(\kappa_x,I_y\kappa_y,I_\omega\omega)\end{pmatrix}$$

$$A_{21}(\kappa_x,I_y\kappa_y,I_\omega\omega)=\begin{pmatrix}\kappa_x x+I_y\kappa_y y+\psi_1(\kappa_x,I_y\kappa_y,I_\omega\omega)+\\ \alpha_{21}(\kappa_x,I_y\kappa_y,I_\omega\omega)\end{pmatrix} \tag{5.2-2b}$$

$$A_{22}(\kappa_x,I_y\kappa_y,I_\omega\omega)=(\kappa_x x+I_y\kappa_y y+\psi_2(\kappa_x,I_y\kappa_y,I_\omega\omega))$$

The three hold integrals can be approximately expressed as (see Chapter 4)

$$f^{(1)}(x,y,t)=\sum_{k=1}^{K}\sum_{n=1}^{N}\sum_{m=1}^{M}\times$$
$$2\sum_{I_y,I_\omega=\pm1}\begin{pmatrix}|\,a_{11}(\kappa_{xn},I_y\kappa_{ym},I_\omega\omega_k)\,|\sqrt{d\kappa_x d\kappa_y d\omega}\times\\ \cos A_{11}(\kappa_{xn},I_y\kappa_{ym},I_\omega\omega_k)\end{pmatrix} \tag{5.2-3a}$$

$$A_{11}(\kappa_{xn},I_y\kappa_{ym},I_\omega\omega_k)=(\kappa_{xn}x+I_y\kappa_{ym}y+\psi_1(\kappa_{xn},I_y\kappa_{ym},I_\omega\omega_k))$$

and

$$g^{(1)}(x,y,t)=\sum_{k=1}^{K}\sum_{n=1}^{N}\sum_{m=1}^{M}\times$$
$$2\sum_{I_y,I_\omega=\pm1}\begin{pmatrix}|\,a_{21}(\kappa_{xn},I_y\kappa_{ym},I_\omega\omega_k)\,|\sqrt{d\kappa_x d\kappa_y d\omega}\times\\ \cos A_{21}(\kappa_{xn},I_y\kappa_{ym},I_\omega\omega_k)+\\ \\ |\,a_{22}(\kappa_{xn},I_y\kappa_{yn},I_\omega\omega_k)\,|\sqrt{d\kappa_x d\kappa_y d\omega}\times\\ \cos A_{22}(\kappa_{xn},I_y\kappa_{ym},I_\omega\omega_k)\end{pmatrix} \tag{5.2-3b}$$

$$A_{21}(\kappa_{xn},I_y\kappa_{ym},I_\omega\omega_k)=\begin{pmatrix}\kappa_{xn}x+I_y\kappa_{ym}y+\psi_1(\kappa_{xn},I_y\kappa_{ym},I_\omega\omega_k)+\\ \alpha_{21}(\kappa_{xn},I_y\kappa_{ym},I_\omega\omega_k)\end{pmatrix}$$

$$A_{22}(\kappa_{xn},I_y\kappa_{ym},I_\omega\omega_k)=(\kappa_{xn}x+I_y\kappa_{ym}y+\psi_2(\kappa_{xn},I_y\kappa_{ym},I_\omega\omega_k))$$

$$\begin{aligned}
&d\kappa_x = \frac{2\kappa_{x\max}}{N}, \quad d\kappa_y = \frac{2\kappa_{x\max}}{M}, \quad d\omega = \frac{2\omega_{\max}}{K} \\
&\kappa_{xn} = nd\kappa_x, \quad \kappa_{yn} = md\kappa_y, \quad \omega_k = kd\omega
\end{aligned} \tag{5.2-3c}$$

where $(\kappa_{x\max}, \kappa_{y\max}, \omega_{\max})$ mean the upper frequency wave numbers in which the frequency wave number power spectral density functions could be zero over them.

6. NUMERICAL EXAMPLES

To visually illustrate the significance of the simulation equations previously described, we present here several numerical examples of the sample function (real value) of $f(x,y) = f^{(1)}(x,y)$ simulated using the simulation equations in Chapter 4. And also, we present here an example of the seismic ground deformation pattern $u(x,y,t_0)$ of ground surface at time $t = t_0$ estimated from seismic observation in Taiwan (SMART-1 Array). By extending the power spectral density function of $u(x,y,t_0)$ estimated from the data of the SMART-1, we demonstrate the temporal space variation of $u(x,y,t)$.

6.1 Simulation Examples

For simplicity, consider the simulation of $f^{(1)}(x,y)$ using Eq. (4.12a) (Quadrant symmetry, Uni-variate, Two-dimensional Case). From Eqs. (4.10c) and (4.12a):

$$f^{(1)}(x,y) = \sqrt{2}\sum_{n=1}^{N}\sum_{m=1}^{M}\left(\begin{array}{l}\sqrt{2S_{ff}(\kappa_{xn},\kappa_{ym})d\kappa_x d\kappa_y} \times \\ \left(\begin{array}{l}\cos(\kappa_{xn}x + \kappa_{ym}y + \psi_{1nm}) + \\ \cos(\kappa_{xn}x - \kappa_{ym}y + \psi'_{1nm})\end{array}\right)\end{array}\right) \tag{6.1-1a}$$

where ψ_{1nm} and ψ'_{1nm} are mutually independent random phase angles uniformly distributed between 0 and 2π. The discrete parameters are given by

$$d\kappa_x = \frac{2\kappa_{x\max}}{N}, \quad d\kappa_y = \frac{2\kappa_{x\max}}{M} \tag{6.1-1b}$$
$$\kappa_{xn} = nd\kappa_x, \quad \kappa_{yn} = md\kappa_y$$

where $(\kappa_{x\max}, \kappa_{y\max})$ mean the upper frequency wave numbers in which the frequency wave number power spectral density functions could be zero over them.

Equation (6.1-1) signifies that a sample function $f^{(1)}(x,y)$ can be expressed as the sum of many elementary waves $\cos(\kappa_{xn}x + \kappa_{ym}y + \psi_{1nm})$ and $\cos(\kappa_{xn}x - \kappa_{ym}y + \psi'_{1nm})$ which propagate in the A and B directions, as shown previously in Fig. 4.1 with amplitude $2\sqrt{S_{ff}(\kappa_{xn}, \kappa_{ym})d\kappa_x d\kappa_y}$. To illustrate the above, two sample functions are generated using only the first term of Eq. (6.1-1a).

In Fig. 6.1-1a, a sample function of $f^{(1)}(x,y)$ is plotted for an isotropic power spectral density function (see Fig. 6.1-2) such as

$$S_{ff}(\kappa) = \sigma^2 \frac{b^2}{4\pi} \exp(-(b\kappa / 2)^2), \quad \kappa = \sqrt{\kappa_x^2 + \kappa_y^2} \tag{6.1-2a}$$

For the numerical example, the following data are used:

$$\sigma = 1, \quad b = 1, \quad N = M = 64, \quad \kappa_{\max} = 2\pi \tag{6.1-2b}$$

From Fig. 6.1-1a, a sample function exhibits an isotropic pattern where the variation pattern is independent of direction. However, if we use only the first term in Eq. (6.1-1a) for the simulation (First Quadrant Symmetry Case), a directional dependent pattern as shown in Fig. 6.1-1b is observed, notwithstanding the use of an isotropic power spectral density function.

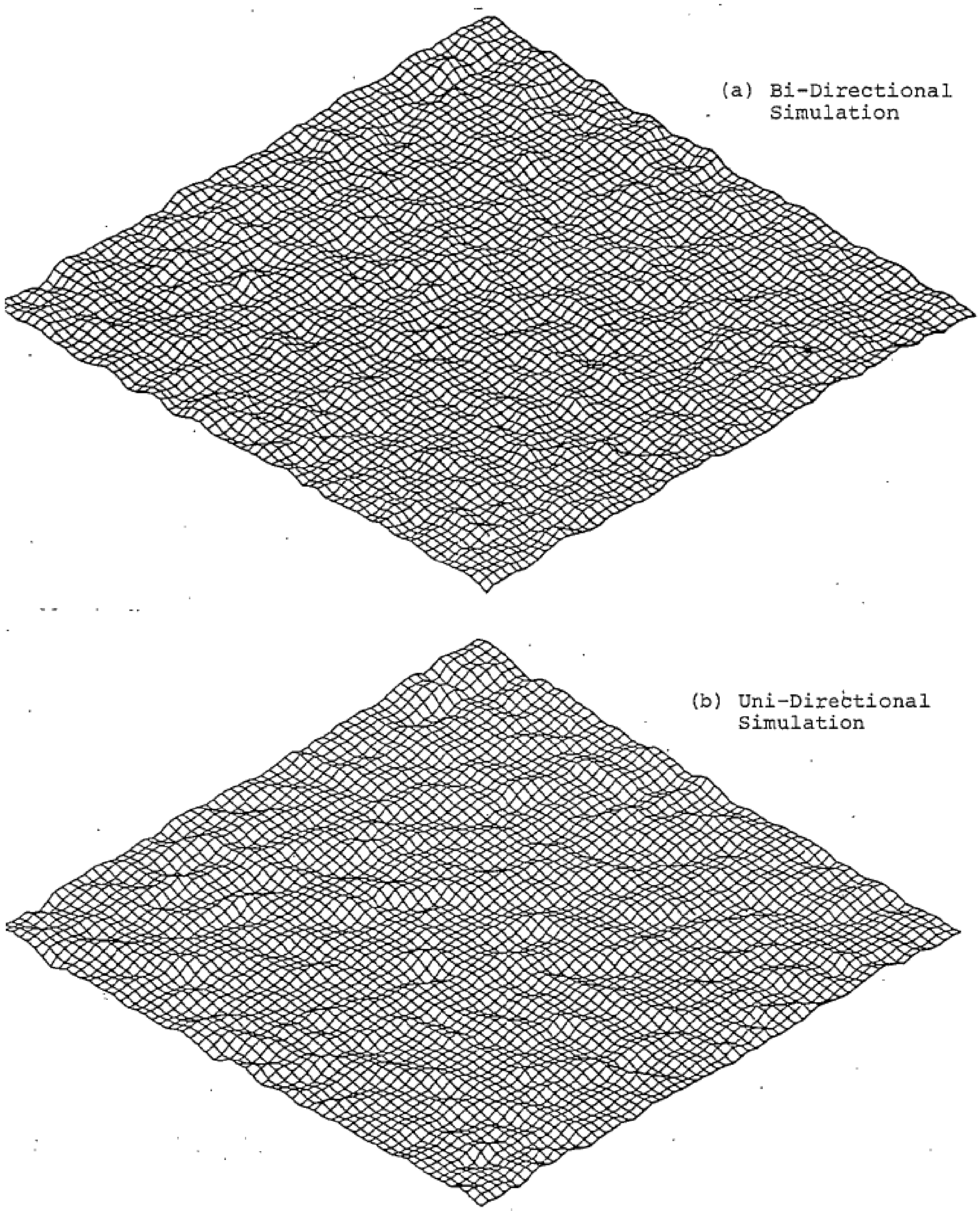

Fig. 6.1-1 Simulated Sample Stochastic Field
((a): Bi-Directional Simulation, (b): Uni-Directional Simulation)

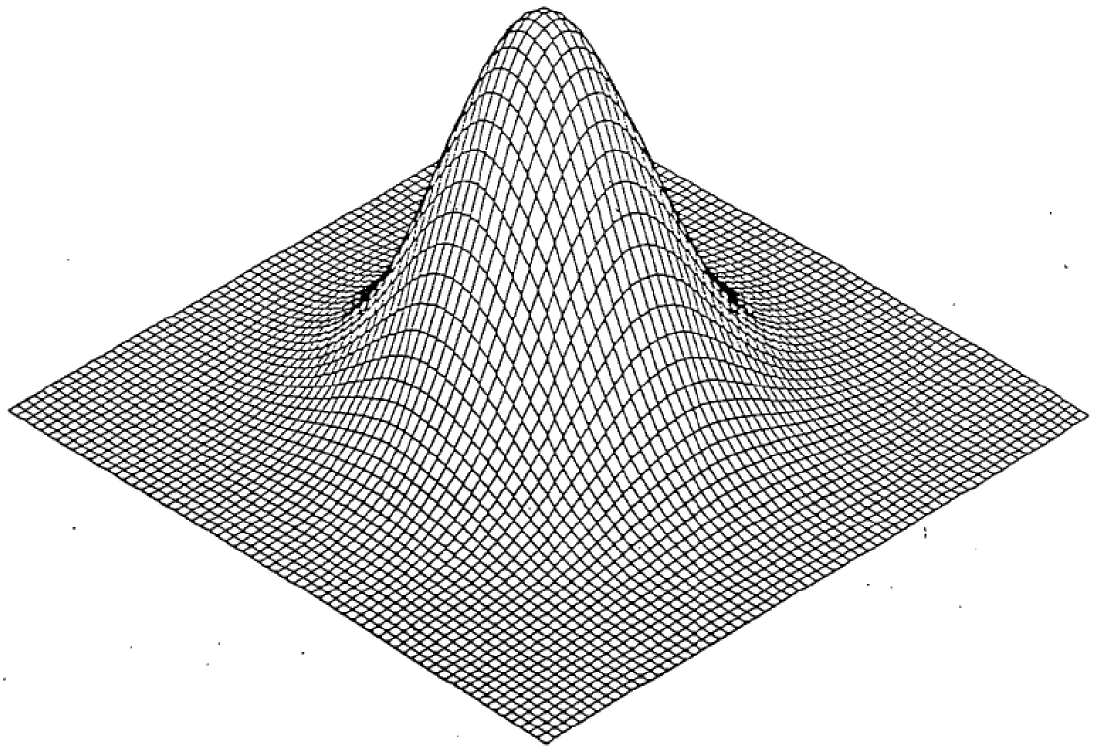

Fig. 6.1-2 Isotropic Spectral Density Function

6.2 Ground Deformation Using Seismic Array Observations

The data used in this study consist of the original accelerograms recorded on January 29, 1981 (Event 5) by a SMART-1 seismograph array as shown in Fig. 6.2-1 installed at Lotung, Taiwan. In this study, a displacement time history along the direction ($\phi = 77^\circ$ or $N13^\circ W$) which is considered to be approximately the direction of the seismic source of this earthquake (Event 5), is computed at each accelerogram station from two-component data (EW and NS). The purpose of this study is to show an example of the spatial variation of seismic ground displacement for the analysis of underground pipelines. A more detailed description of this study is given in a report by Harada and Oda (1984).

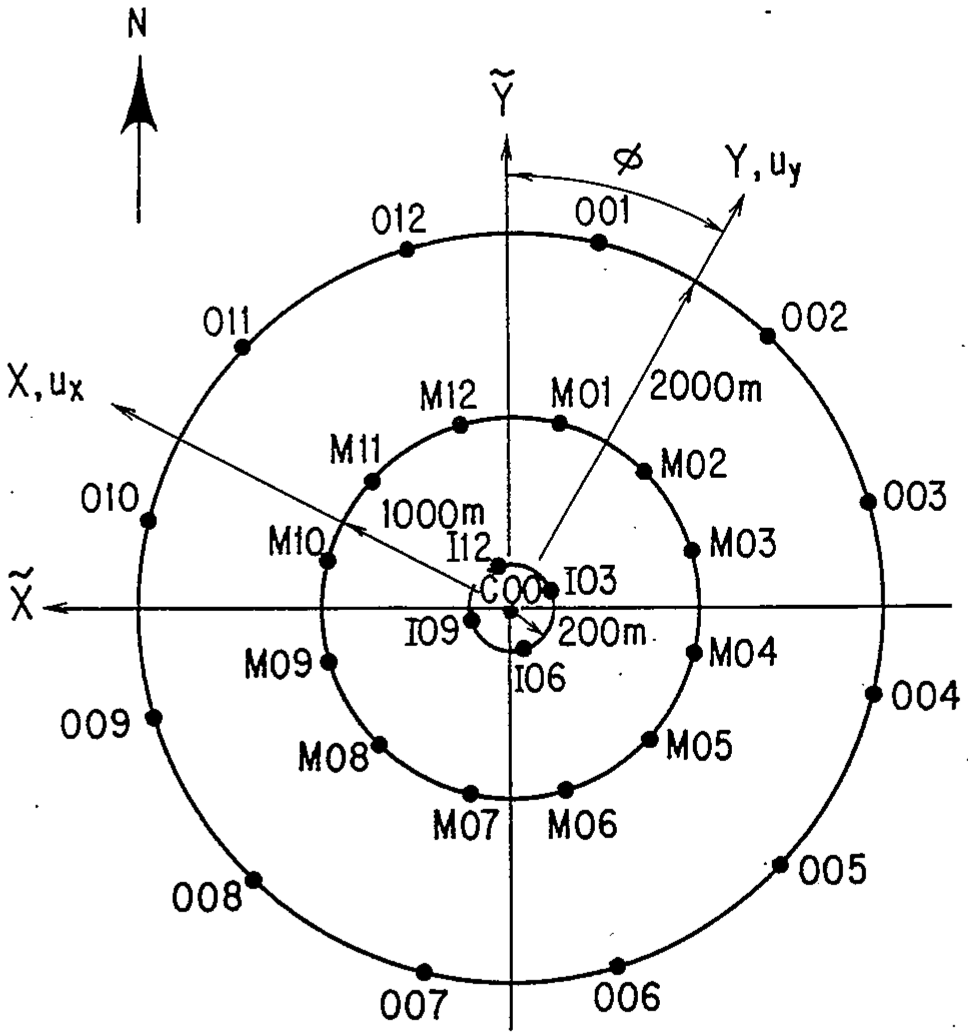

Fig. 6.2-1 The SMART-1 Array and Coordinate System

By interpreting the displacement time history $u(x,y,t)$ ($N13°W$ component) at each station as sample functions of the uni-variate and spatially two-dimensional time-space stochastic process $f^{(1)}(x,y,t)$, and using Eq. (5.1-9a), a spatial correlation function $B_{uu}(\xi_x,\xi_y)$ was computed from the records of all the combinations of the 17 stations, C-00, I-03~I-12, M-03~M-09 and O-04~O-09, specifying the standard stations as C-00, M-05 and O-05. Since the computed correlation functions approximately indicate quadrant symmetric behavior, that is, ($B_{uu}(\xi_x,\xi_y)=B_{uu}(\xi_x,-\xi_y)$), all the correlation coefficient data were plotted by alim arrows as shown in Fig. 6.2-2.

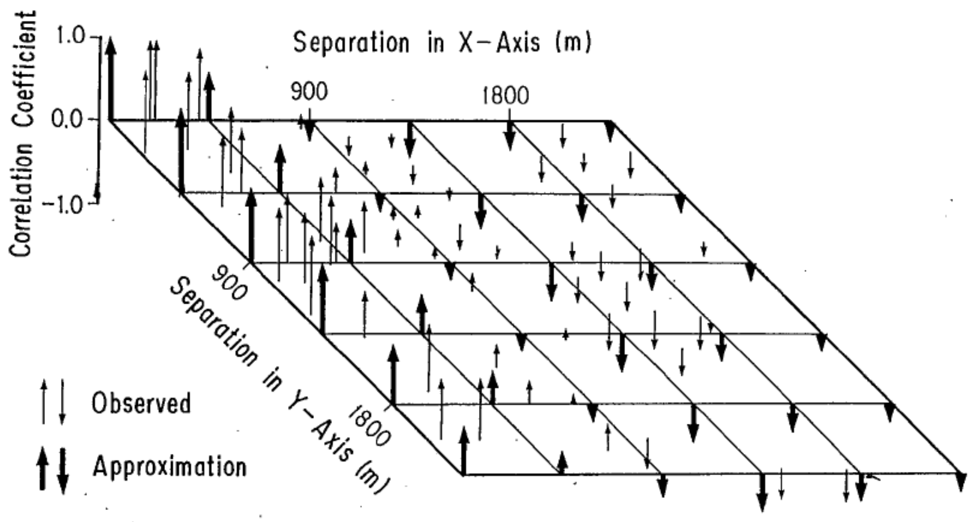

Fig. 6.2-2 Observed and Approximated Two Dimensional Correlations

By judging the distribution of the correlation coefficients, a simple analytical correlation function was assumed such that

$$B_{uu}(\xi_x, \xi_y) = \sigma_{uu}^2 \left(1 - 2\left(\frac{\xi_x}{b_x}\right)^2\right) \exp\left(-\left(\frac{\xi_x}{b_x}\right)^2 - \left(\frac{\xi_y}{b_y}\right)^2\right) \tag{6.2-1a}$$

where $\sigma_{uu} = 1.24\,\mathrm{cm}, b_x = 1.131 \times 10^3\,\mathrm{m}, b_y = 3.012 \times 10^3\,\mathrm{m}$. The values of Eq. (6.2-1) are also plotted with fat arrows in Fig. 6.2-2 indicating that the analytical form of Eq. (6.2-1a) is approximately valid. From the Wiener Khintchine relationship shown in Fig. 5.1-1, the corresponding power spectral density function $S_{uu}(\kappa_x, \kappa_y)$ is obtained as

$$\begin{aligned} S_{uu}(\kappa_x, \kappa_y) &= \frac{1}{(2\pi)^2} \int_{-\infty}^{\infty} \int_{-\infty}^{\infty} B_{uu}(\xi_x, \xi_y) e^{i(\kappa_x \xi_x + \kappa_y \xi_y)} d\xi_x d\xi_y \\ &= \frac{\sigma_{uu}^2}{8\pi} b_x^3 b_y \kappa_x^2 \exp\left(-\left(\frac{b_x \kappa_x}{2}\right)^2 - \left(\frac{b_y \kappa_y}{2}\right)^2\right) \end{aligned} \tag{6.2-1b}$$

A sample function of $u(x, y)$ in the area of 22747.60 m by 19884.06 m is shown in Fig. 6.2-3. In this example, following data are used in Eq. (6.1-1):

$$\begin{aligned} &N = M = 64 \\ &\kappa_{x\max} = 10 / b_x = 8.84 \times 10^{-3}\,\mathrm{rad/m} \\ &\kappa_{y\max} = 10 / b_y = 3.32 \times 10^{-3}\,\mathrm{rad/m} \end{aligned} \tag{6.1-1c}$$

It is observed from Fig. 6.2-3 that there is relatively rapid variation along the x axis ($N13^\circ W$: seismic source approximate direction) compared with the variation along the y axis. From the number of peaks (9) along the x axis (22747.60 m) in Fig. 6.2-3, the apparent wave length along the x axis is estimated to be about 2.5 km. Hence, the pattern in Fig. 6.2-3 indicates that a single wave with a wavelength of approximately 2.5 km propagates in the x direction. In fact, for Event 5 data, the other study shows that a strong portion of the records consist of a wave with frequency of approximately 1.2 Hz and that it propagates in the x direction with a speed of about 3 km/s (Bolt, et.al. (1982)) indicating a wavelength of 2.5 km (3/1.2). This result is quite consistent with the variation pattern shown in Fig. 6.2-3.

In Fig. 6.2-3, the correlation distance (1897.4 m) means the length where the correlation of stochastic fields is very high (Harada and Shinozuka (1986)).

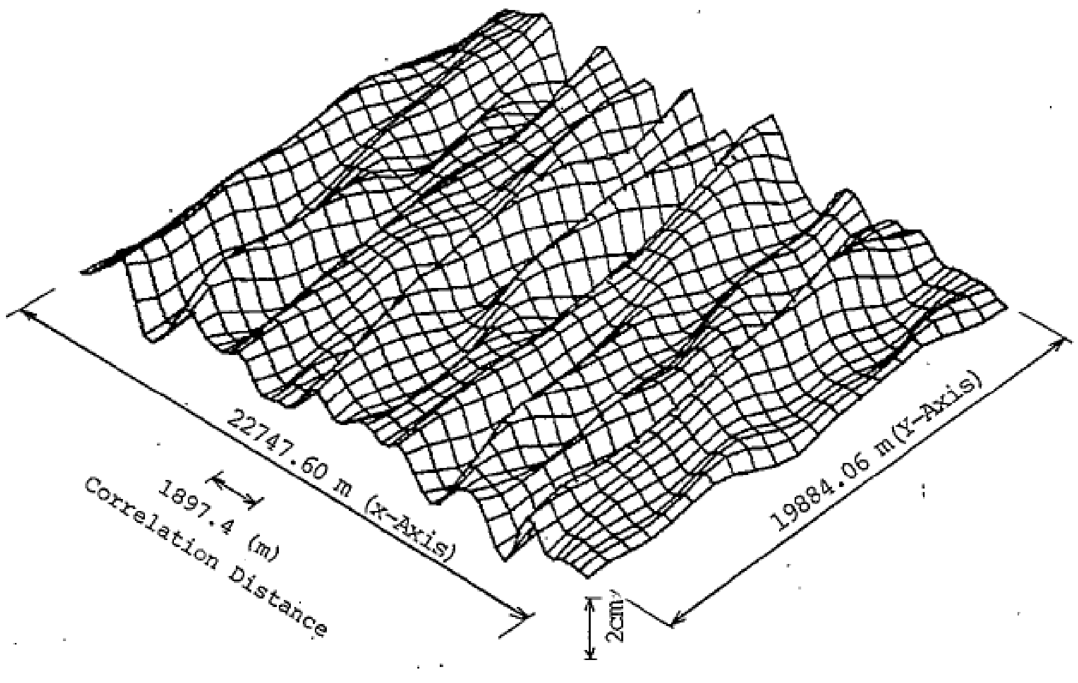

Fig. 6.2-3 A Sample Function of $u(x,y)$ (Event 5, SMART-1 Array)

6.3 Spatially Two Dimensional Homogeneous Non-Stationary Stochastic Wave

By extending the two-dimensional power spectral density function $S_{uu}(\kappa_x, \kappa_y)$ given by Eq. (6.2-1b) in conjunction with the wave propagation, the power spectral density function of $u(x, y, t)$ may be modelled such that

$$\begin{aligned} &S_{uu}(\kappa_x, \kappa_y, \omega) = S_{uu}(\kappa_x, \kappa_y)\delta(\omega - g(\kappa_x, \kappa_y)) \\ &g(\kappa_x, \kappa_y) = C\kappa = C\sqrt{\kappa_x^2 + \kappa_y^2} \end{aligned} \tag{6.3-1}$$

where C is the speed of wave propagation and we assume here $C = 640\,\mathrm{m/s}$ for an example of simulation of $u(x, y, t)$. Due to the wave propagation, the frequency is related with the wave numbers such as $\omega = C\kappa$ that is, the frequency is determined by the wave numbers. In this model, the predominant frequency is approximately 0.26Hz (=640/2500) because the wavelength of x direction is about 2.5km from Section 6.2 or Fig. 6.2-3. It is noted here that if we assume $C = 3{,}000\,\mathrm{m/s}$, the predominant frequency is about 1.2Hz (3000/2500) as the observed data of Event 5.

We introduce the evolutionary power spectrum $S_{uu}(\kappa_x, \kappa_y, \omega, t)$ of a spatially two-dimensional homogeneous, non-stationary stochastic wave as

$$S_{uu}(\kappa_x, \kappa_y, \omega, t) = |A(\omega, t)|^2\, S_{uu}(\kappa_x, \kappa_y, \omega) \tag{6.3-2a}$$

For this example, the modulating function $A(\omega, t)$ is assumed as

$$A(\omega, t) = \frac{\exp(-0.25t) - \exp(-(0.3765\omega + 0.251)t)}{\exp(-0.25t^*) - \exp(-(0.3765\omega + 0.251)t^*)} \tag{6.3-2b}$$

where t^* indicate the time instant at which assume a maximum value as a function of time;

$$t^* = \frac{\ln(0.3765\omega + 0.251) - \ln 0.25}{0.3765\omega + 0.001} \tag{6.3-2c}$$

Figure 6.3-1 shows the modulating function used in this numerical example indicating the higher frequency is predominant in the early time, while the lower frequency is involved in the later time.

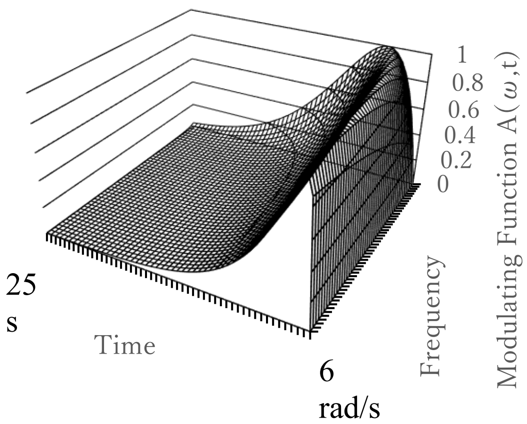

Fig. 6.3-1 Modulating Function $A(\omega,t)$

Similar to Eq. (6.1-1), the spatially two-dimensional homogeneous non-stationary stochastic wave can be simulated using the following expression,

$$u(x,y,t) = \sqrt{2}\sum_{n=1}^{N}\sum_{m=1}^{M}\left(\begin{array}{l}\sqrt{2\mid A(t,g(\kappa_{xn},\kappa_{ym}))\mid^2 S_{uu}(\kappa_{xn},\kappa_{ym})d\kappa_x d\kappa_y} \times \\ \left(\begin{array}{l}\cos(\kappa_{xn}x + \kappa_{ym}y - g(\kappa_{xn},\kappa_{ym})t + \psi_{1nm}) + \\ \cos(\kappa_{xn}x - \kappa_{ym}y - g(\kappa_{xn},\kappa_{ym})t + \psi'_{1nm})\end{array}\right)\end{array}\right) \tag{6.3-3}$$

where the same parameters given by Eq. (6.1-1c) are used.

The stochastic wave is now simulated, using Eq. (6.3-3), over a 10 km by 10 km area as shown in Fig. 6.3-2.

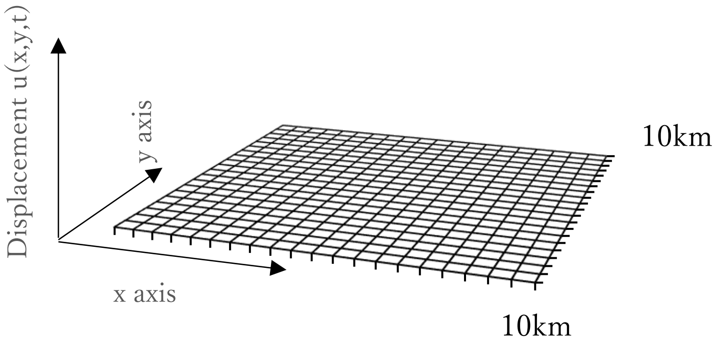

Fig. 6.3-2 Simulated Area

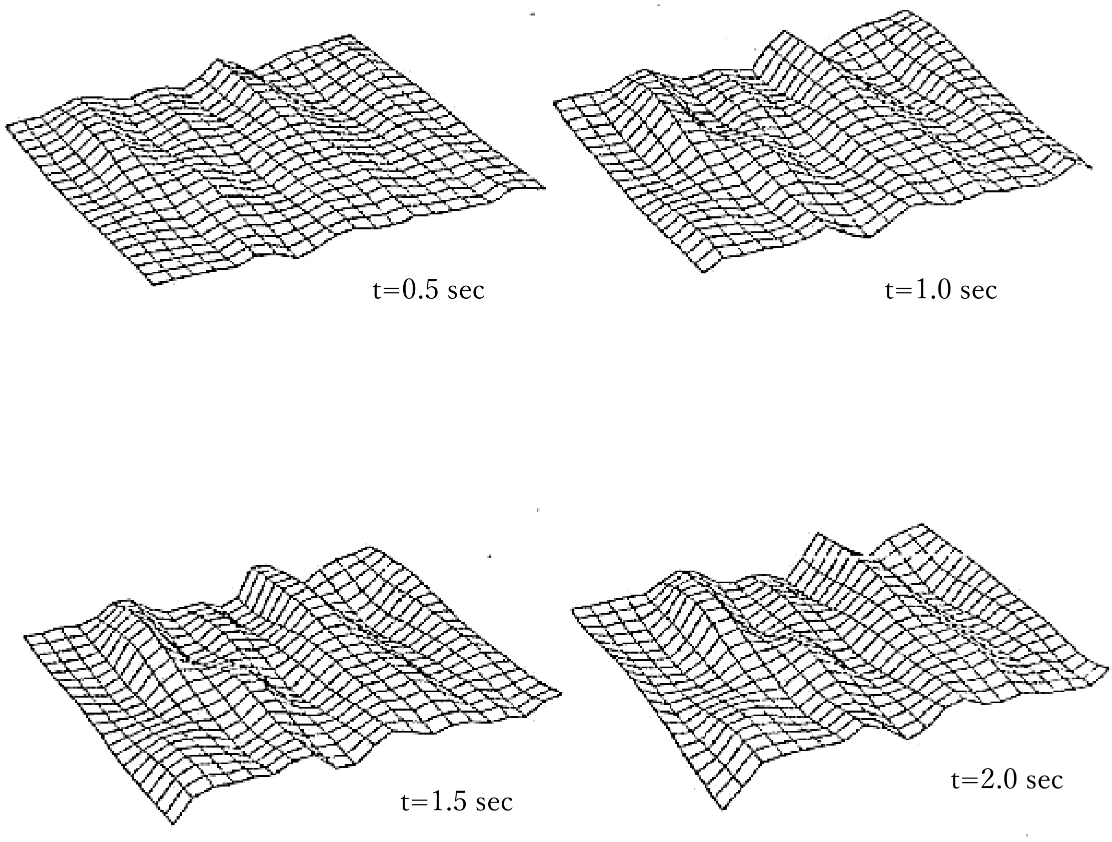

Fig. 6.3-2 Simulated Stochastic Wave at 4 Equispaced Time Instants

The simulation is performed at 12 equispaced time instants, 0.5 sec apart from each other, and shown in Fig. 6.3-3 at 4 equispaced time instants.

It is clearly observed in 4 plots that there is relatively rapid variation along the x axis compared to the variation along the y axis, as shown in Fig. 6.2-3 previously. From the number of peaks (4) along the x axis, the apparent wave length along this axis is estimated to be around 2.5 km similar to that of Fig. 6.2-3.

7. ESTIMATION OF SPECTRAL DENSITY FUNCTION

In the previous Chapters 5 and 6, the spectral representation of stochastic fields and the numerical examples are presented if the power spectral density function are given. Hence the estimation of the power spectral density function is necessary to simulate the stochastic fields. In this Chapter, the estimation method of the power spectral density function from a set of discrete data equally spaced (1) one-dimensional case, (2) two-dimensional case, and (3) a set of discrete time space data not equally spaced such as a seismic array data where the many seismographs are usually installed on the ground surface not equally spaced.

7.1 Bi-Variate, One-Dimensional Case

We consider the estimation of a spectral density function from the finite length real valued records $f(x)$ and $g(x)$ with zero mean defined in the range $0 \le x \le L$.

The finite range Fourier transform can be defined such that (Bendat and Piersol (1971)),

$$
\begin{aligned}
&F_j(\kappa, L) = \int_0^L j(x) \mathrm{e}^{-i\kappa x} dx, \qquad j = f, g \\
&j(x) = \frac{1}{2\pi} \int_{-\infty}^{\infty} F_j(\kappa, L) \mathrm{e}^{i\kappa x} d\kappa \\
&F_j(-\kappa, L) = F_j^*(\kappa, L)
\end{aligned}
\tag{7.1-1}
$$

Assuming that $f(x)$ and $g(x)$ are sampled at N equally spaced points with distance $dx = L / N$ apart, then $f(x)$ and $g(x)$ can be expressed as

$$j(n) = j(ndx) \quad n = 1,2,\cdots,N \tag{7.1-2a}$$

For arbitrary κ, the discrete version of Eq. (7.1-1) is

$$F_j(\kappa, L) = dx\sum_{n=1}^{N} j(n)\mathrm{e}^{-i\kappa ndx} \tag{7.1-2b}$$

The usual selection of a discrete wave number for the computation of $F_j(\kappa, L)$ is

$$\kappa_p = p\frac{2\pi}{L} = p\frac{2\pi}{Ndx} = pd\kappa, \quad p = 1,2,\cdots,N \tag{7.1-3a}$$

At these wave numbers, Eq. (7.1-2b) can be written as

$$F_j(\kappa_p, L) = dx\sum_{n=1}^{N} j(n)\mathrm{e}^{-i\frac{2\pi pn}{N}}, \quad p = 1,2,\cdots,N \tag{7.1-3b}$$

On the other hand, for large L, the covariance function may be estimated by

$$\begin{aligned} R_{jk}(\xi) &= \frac{1}{L}\int_{0}^{L-\xi} j(x+\xi)k(x)dx, \quad 0 \le \xi \le L \\ R_{jk}(\xi) &= \frac{1}{L}\int_{-\xi}^{L} j(x+\xi)k(x)dx, \quad -L \le \xi \le 0 \end{aligned} \tag{7.1-4a}$$

Recalling the Wiener Khintchine relationships, the power spectral density function $S_{jk}(\kappa)$ may also be estimated by

$$S_{jk}(\kappa) = \frac{1}{2\pi}\int_{-L}^{L} R_{jk}(\xi)\mathrm{e}^{-i\kappa\xi}d\xi \tag{7.1-4b}$$

Equation (7.1-4b) is also written substituting Eq. (7.1-4a) into Eq. (7.1-4b) as

$$S_{jk}(\kappa) = \frac{1}{2\pi L}\left(\int_{-L}^{0}\left(\int_{-\xi}^{L} j(x+\xi)k(x)dx\right)e^{-i\kappa\xi}d\xi\right) + \frac{1}{2\pi L}\left(\int_{0}^{L}\left(\int_{0}^{L-\xi} j(x+\xi)k(x)dx\right)e^{-i\kappa\xi}d\xi\right) \tag{7.1-4c}$$

By changing the region of integration as shown schematically in Fig. 7.1-1 from $(0 \le x \le L, -L \le \xi \le L)$ to $(0 \le x \le L, 0 \le \beta \le L)$ where $\beta = x + \xi$, and $d\xi = d\beta$, the above integral can be expressed as

$$\int_{-L}^{0}\int_{-\xi}^{L} dxd\xi + \int_{0}^{L}\int_{0}^{L-\xi} dxd\xi = \int_{0}^{L}\int_{0}^{L} dxd\beta \tag{7.1-5}$$

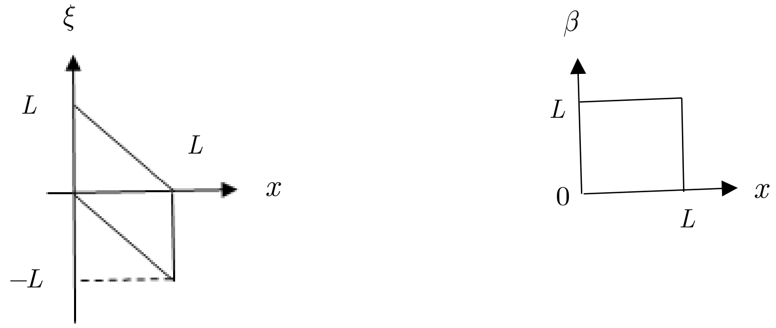

(a) (x,ξ) Region (b) (x,β) Region

Fig. 7.1-1 Region of Integration

Hence, Eq. (7.1-4c) becomes, accounting from Eq. (7.1-5), such that

$$S_{jk}(\kappa) = \frac{1}{2\pi L}\int_{0}^{L} j(\beta)e^{-i\kappa\beta}d\beta \int_{0}^{L} k(x)e^{i\kappa x}dx \tag{7.1-6a}$$

Recalling Eq. (7.1-1), Eq. (7.1-6a) can also be expressed as

$$S_{jk}(\kappa) = \frac{1}{2\pi L}F_j(\kappa, L)F_k^*(\kappa, L) \tag{7.1-6b}$$

At the discrete wave number, Eq. (7.1-6) is expressed using Eq. (7.1-3b) as follows:

$$S_{jk}(\kappa_p = pd\kappa) = \frac{1}{d\kappa}\left(\left(\frac{1}{N}\sum_{n=1}^{N} j(n)\mathrm{e}^{-i\frac{2\pi pn}{N}}\right)\left(\frac{1}{N}\sum_{n=1}^{N} k(n)\mathrm{e}^{i\frac{2\pi pn}{N}}\right)\right) \quad (7.1\text{-}7a)$$

If $j = k$, Eq. (7.1-7a) reduces to

$$S_{jj}(\kappa_p = pd\kappa) = \frac{1}{d\kappa}\left|\frac{1}{N}\sum_{n=1}^{N} j(n)\mathrm{e}^{-i\frac{2\pi pn}{N}}\right|^2 \quad (7.1\text{-}7b)$$

Equation (7.1-7) are suitable for the estimation of the power spectral density function via finite Fourier transforms using the Fast Fourie Transform (FFT) technique.

7.2 Bi-Variate, Two-Dimensional Case

Using the procedures similar to those for the bi-variate, one-dimensional case described in the previous section, we describe the estimation of the power spectral density function for the bi-variate, two-dimensional, real valued stochastic fields $f(x,y)$ and $g(x,y)$, defined in the finite regions $0 \le x \le L_x$ and $0 \le y \le L_y$.

Finite range Fourier transform for the two-dimensional case can be defined such that

$$F_j(\kappa_x, \kappa_y, L_x, L_y) = \int_0^{L_x}\int_0^{L_y} j(x,y) e^{-i(\kappa_x x + \kappa_y y)} dxdy, \quad j = f, g$$

$$j(x,y) = \frac{1}{(2\pi)^2} \int_{-\infty}^{\infty}\int_{-\infty}^{\infty} F_j(\kappa_x, \kappa_y, L_x, L_y) e^{i(\kappa_x x + \kappa_y y)} d\kappa_x d\kappa_y \tag{7.2-1}$$

$$F_j(-\kappa_x, -\kappa_y, L_x, L_y) = F_j^*(\kappa_x, \kappa_y, L_x, L_y)$$

and, at discrete wave numbers and locations, Eq. (7.2-1) can be expressed as

$$F_j(\kappa_{xp}, \kappa_{yq}, L_x, L_y) = dxdy \sum_{n=1}^{N}\sum_{m=1}^{M} j(n,m) e^{-i\left(\frac{2\pi pn}{N} + \frac{2\pi qm}{M}\right)} \tag{7.2-2a}$$

where $p = 1, 2, \cdots, N, q = 1, 2, \cdots, M$ and

$$\begin{aligned} dx &= \frac{L_x}{N}, \quad dy = \frac{L_y}{M} \\ \kappa_{xp} &= p\frac{2\pi}{L_x} = p\frac{2\pi}{Ndx} = pd\kappa_x \\ \kappa_{yq} &= q\frac{2\pi}{L_y} = q\frac{2\pi}{Mdy} = qd\kappa_y \end{aligned} \tag{7.2-2b}$$

For large L_x, L_y, the covariance function $R_{jk}(\xi_x, \xi_y)$ may also be estimated by

For $0 \le \xi_x \le L_x$ and $0 \le \xi_y \le L_y$:

$$R_{jk}(\xi_x, \xi_y) = \frac{1}{L_x L_y} \int_0^{L_x - \xi_x}\int_0^{L_y - \xi_y} j(x + \xi_x, y + \xi_y) k(x,y) dxdy \tag{7.2-3a}$$

For $-L_x \le \xi_x \le 0$ and $0 \le \xi_y \le L_y$:

$$R_{jk}(\xi_x, \xi_y) = \frac{1}{L_x L_y} \int_{-\xi_x}^{L_x}\int_0^{L_y - \xi_y} j(x + \xi_x, y + \xi_y) k(x,y) dxdy \tag{7.2-3b}$$

For $-L_x \le \xi_x \le 0$ and $-L_y \le \xi_y \le 0$:

$$R_{jk}(\xi_x, \xi_y) = \frac{1}{L_x L_y} \int_{-\xi_x}^{L_x} \int_{-\xi_y}^{L_y} j(x+\xi_x, y+\xi_y) k(x,y) dx dy \tag{7.2-3c}$$

For $0 \le \xi_x \le L_x$ and $-L_y \le \xi_y \le 0$:

$$R_{jk}(\xi_x, \xi_y) = \frac{1}{L_x L_y} \int_{0}^{L_x-\xi_x} \int_{-\xi_y}^{L_y} j(x+\xi_x, y+\xi_y) k(x,y) dx dy \tag{7.2-3d}$$

Recalling the Wiener Khintchine relationships, the power spectral density function $S_{jk}(\kappa_x, \kappa_y)$ may be estimated by

$$S_{jk}(\kappa_x, \kappa_y) = \frac{1}{(2\pi)^2} \int_{-L_x}^{L_x} \int_{-L_y}^{L_y} R_{jk}(\xi_x, \xi_y) \mathrm{e}^{-i(\kappa_x \xi_x + \kappa_y \xi_y)} d\xi_x d\xi_y \tag{7.2-4}$$

Substituting Eq. (7.2-3) into Eq. (7.2-4) and taking into account the following relationship similar to Eq. (7.1-5) with $\beta_x = x + \xi_x, \beta_y = y + \xi_y$,

$$\begin{aligned}
&\int_0^{L_x}\int_0^{L_y}\int_0^{L_x}\int_0^{L_y} dx dy d\beta_x d\beta_y = \int_0^{L_x}\int_0^{L_x} dx d\beta_x \int_0^{L_y}\int_0^{L_y} dy d\beta_y \\
&= \left(\int_{-L_x}^{0} \int_{-\xi_x}^{L_x} dx d\xi_x + \int_{0}^{L_x} \int_{0}^{L_x-\xi_x} dx d\xi_x \right) \times \left(\int_{-L_y}^{0} \int_{-\xi_y}^{L_y} dy d\xi_y + \int_{0}^{L_y} \int_{0}^{L_y-\xi_y} dy d\xi_y \right) \\
&= \left(\int_{-L_x}^{0} \int_{-L_y}^{0} \int_{-\xi_x}^{L_x} \int_{-\xi_y}^{L_y} dx dy d\xi_x d\xi_y + \int_{-L_x}^{0} \int_{0_y}^{L_y} \int_{-\xi_x}^{L_x} \int_{0}^{L_y-\xi_y} dx dy d\xi_x d\xi_y \right) + \\
&\left(\int_{0}^{L_x} \int_{-L_y}^{0} \int_{0}^{L_x-\xi_x} \int_{-\xi_y}^{L_y} dx dy d\xi_x d\xi_y + \int_{0}^{L_x} \int_{0}^{L_y} \int_{0}^{L_x-\xi_x} \int_{0}^{L_y-\xi_y} dx dy d\xi_x d\xi_y \right)
\end{aligned} \tag{7.2-5}$$

Equation (7.2-4) is also expressed as

$$S_{jk}(\kappa_x,\kappa_y)=\frac{1}{(2\pi)^2 L_x L_y}\left(\begin{array}{l}\displaystyle\int_0^{L_x}\int_0^{L_y} j(\beta_x,\beta_y)\mathrm{e}^{-i(\kappa_x\beta_x+\kappa_y\beta_y)}d\beta_x d\beta_y\times\\ \displaystyle\int_0^{L_x}\int_0^{L_y} k(x,y)\mathrm{e}^{-i(\kappa_x x+\kappa_y y)}dxdy\end{array}\right)\tag{7.2-6a}$$

Substitution of Eq. (7.2-2a) into Eq. (7.2-6a) yields

$$S_{jk}(\kappa_x,\kappa_y)=\frac{1}{(2\pi)^2 L_x L_y}F_j(\kappa_x,\kappa_y,L_x,L_y)F_k^*(\kappa_x,\kappa_y,L_x,L_y)\tag{7.2-6b}$$

At the discrete wave number, Eq. (7.2-6b) is expressed using Eq. (7.2-2) as follows:

$$S_{jk}(\kappa_{xp},\kappa_{yq})=\frac{1}{d\kappa_x d\kappa_y}\left(\begin{array}{l}\left(\displaystyle\frac{1}{NM}\sum_{n=1}^{N}\sum_{m=1}^{M} j(n,m)\mathrm{e}^{-i\left(\frac{2\pi pn}{N}+\frac{2\pi qm}{M}\right)}\right)\times\\ \left(\displaystyle\frac{1}{NM}\sum_{n=1}^{N}\sum_{m=1}^{M} k(n,m)\mathrm{e}^{i\left(\frac{2\pi pn}{N}+\frac{2\pi qm}{M}\right)}\right)\end{array}\right)\tag{7.2-7a}$$

If $j=k$, Eq. (7.1-7a) reduces to

$$S_{jj}(\kappa_{xp},\kappa_{yq})=\frac{1}{d\kappa_x d\kappa_y}\left|\frac{1}{NM}\sum_{n=1}^{N}\sum_{m=1}^{M} j(n,m)\mathrm{e}^{-i\left(\frac{2\pi pn}{N}+\frac{2\pi qm}{M}\right)}\right|^2\tag{7.2-7b}$$

By utilizing Eq. (7.2-7) together with the FFT technique, the power spectral density function $S_{jj}(\kappa_{xp},\kappa_{yq})$ can be efficiently estimated from a set of discrete data equally spaced $dx=L_x/N, dy=L_y/M$ in the region $0\le x\le L_x$ and $0\le y\le L_y$.

7.3 One-Variate, Time Space Ground Surface Array Data

We consider now the time space function $f(x,y,t)(=f^{(1)}(x,y,t))$ as the observed seismic array records. These records are not usually observed in equally spaced array. Herein, we describe the two estimation methods of the power spectral density function from the array data; (1) Conventional method and (2) High resolution method by Capon (1969, 1973).

In this section, the real valued continuous time space function $f(\boldsymbol{x},t)(=f(x,y,t)),\boldsymbol{x}=(x,y)$ of finite time $0\le t\le T,$ and finite space regions $0\le \boldsymbol{x}\le \boldsymbol{L}(=0\le x\le L_x, 0\le y\le L_y)$ where $\boldsymbol{L}=(L_x,L_y)$ are expressed such as

$$f(x,y,t)=\begin{cases} 0 & t<0,\boldsymbol{x}<0 \\ f_{T\boldsymbol{L}}(\boldsymbol{x},t) & 0\le t\le T, 0\le \boldsymbol{x}\le \boldsymbol{L} \\ 0 & T<t,\boldsymbol{L}<\boldsymbol{x} \end{cases} \tag{7.3-1a}$$

and the frequency wave number spectrum of $f_{T\boldsymbol{L}}(\boldsymbol{x},t)$ is defined as

$$\begin{aligned} F_{T\boldsymbol{L}}(\boldsymbol{k},\omega) &= \int_{-\infty}^{\infty}\int_{-\infty}^{\infty}\int_{-\infty}^{\infty} f_{T\boldsymbol{L}}(\boldsymbol{x},t)\mathrm{e}^{-i(\boldsymbol{k}\cdot\boldsymbol{x}-\omega t)}d\boldsymbol{x}dt \\ f_{T\boldsymbol{L}}(\boldsymbol{x},t) &= \frac{1}{(2\pi)^3}\int_{-\infty}^{\infty}\int_{-\infty}^{\infty}\int_{-\infty}^{\infty} F_{T\boldsymbol{L}}(\boldsymbol{k},\omega)\mathrm{e}^{i(\boldsymbol{k}\cdot\boldsymbol{x}-\omega t)}d\boldsymbol{k}d\omega \end{aligned} \tag{7.3-1b}$$

where $\boldsymbol{k}=(\kappa_x,\kappa_y)$ and ω mean the wavenumber vector and frequency, and $\boldsymbol{k}\cdot\boldsymbol{x}=\kappa_x x+\kappa_y y$. By the above definitions, the complex conjugate Fourier spectrum is given by

$$F_{TL}^{*}(\boldsymbol{k},\omega)=\int_{-\infty}^{\infty}\int_{-\infty}^{\infty}\int_{-\infty}^{\infty} f_{TL}(\boldsymbol{x},t)\mathrm{e}^{i(\boldsymbol{k}\cdot\boldsymbol{x}-\omega t)}d\boldsymbol{x}dt$$

$$f_{TL}(\boldsymbol{x},t)=\frac{1}{(2\pi)^3}\int_{-\infty}^{\infty}\int_{-\infty}^{\infty}\int_{-\infty}^{\infty} F_{TL}^{*}(\boldsymbol{k},\omega)\mathrm{e}^{-i(\boldsymbol{k}\cdot\boldsymbol{x}-\omega t)}d\boldsymbol{k}d\omega \tag{7.3-1c}$$

(1) Conventional Method

Denoting the observed seismic data $f_n(t)=f(x_n,y_n,t)$ from seismograph located on ground surface $(x_n,y_n), n=1,\cdots N$. Then, these Fourier spectra can be estimated by

$$F_n(\omega)=\int_0^T f_n(t)\mathrm{e}^{i\omega t}dt$$

$$F_n^{*}(\omega)=\int_0^T f_n(t)\mathrm{e}^{-i\omega t}dt \tag{7.3-2a}$$

By defining the vector of these Fourier spectra such as

$$\boldsymbol{F}(\omega)=\begin{pmatrix}F_1(\omega)\\ F_2(\omega)\\ \vdots\\ F_N(\omega)\end{pmatrix},\quad \boldsymbol{F}^{*}(\omega)=\begin{pmatrix}F_1^{*}(\omega)\\ F_2^{*}(\omega)\\ \vdots\\ F_N^{*}(\omega)\end{pmatrix} \tag{7.3-2b}$$

Then the frequency wave number spectrum of continuous time space function $f(x,y,t)=f_{TL}(\boldsymbol{x},t)$ is given approximately by the weighted sum with complex weight W_n such as

$$
\begin{aligned}
F_{T\boldsymbol{L}}(\boldsymbol{k},\omega) &= \sum_{n=1}^{N} W_n F_n(\omega) \mathrm{e}^{-i\boldsymbol{k}\cdot\boldsymbol{x}} \\
F^*_{T\boldsymbol{L}}(\boldsymbol{k},\omega) &= \sum_{n=1}^{N} W^*_n F^*_n(\omega) \mathrm{e}^{i\boldsymbol{k}\cdot\boldsymbol{x}}
\end{aligned}
\tag{7.3-3}
$$

By extending Eq. (7.2-6b) of two-dimensional function, the power spectral density function $S_{T\boldsymbol{L}}(\boldsymbol{k},\omega)$ of time space function $f_{T\boldsymbol{L}}(\boldsymbol{x},t)$ is given by

$$
\begin{aligned}
S_{T\boldsymbol{L}}(\boldsymbol{k},\omega) &= \frac{1}{(2\pi)^3 L_x L_y T} F_{T\boldsymbol{L}}(\boldsymbol{k},\omega) F^*_{T\boldsymbol{L}}(\boldsymbol{k},\omega) \\
&= \frac{1}{(2\pi)^3 L_x L_y T} \sum_{m=1}^{N} \sum_{n=1}^{N} W_m W^*_n F_m(\omega) F^*_n(\omega) \mathrm{e}^{-i\boldsymbol{k}\cdot(\boldsymbol{x}_m - \boldsymbol{x}_n)} \\
&= \frac{1}{(2\pi)^3 L_x L_y T} \left| \boldsymbol{W}\boldsymbol{U}^{*T}(\boldsymbol{k}) \boldsymbol{S}(\omega) \boldsymbol{U}(\boldsymbol{k}) \boldsymbol{W}^{*T} \right|
\end{aligned}
\tag{7.3-4a}
$$

where $\boldsymbol{U}(\boldsymbol{k})$ means the array wave number vector as

$$
\begin{aligned}
&\boldsymbol{W} = \begin{pmatrix} W_1 \\ W_2 \\ \vdots \\ W_N \end{pmatrix}, \quad \boldsymbol{U}(\boldsymbol{k}) = \begin{pmatrix} \mathrm{e}^{i\boldsymbol{k}\cdot\boldsymbol{x}_1} \\ \mathrm{e}^{i\boldsymbol{k}\cdot\boldsymbol{x}_2} \\ \vdots \\ \mathrm{e}^{i\boldsymbol{k}\cdot\boldsymbol{x}_N} \end{pmatrix}, \quad \boldsymbol{U}^*(\boldsymbol{k}) = \begin{pmatrix} \mathrm{e}^{-i\boldsymbol{k}\cdot\boldsymbol{x}_1} \\ \mathrm{e}^{-i\boldsymbol{k}\cdot\boldsymbol{x}_2} \\ \vdots \\ \mathrm{e}^{-i\boldsymbol{k}\cdot\boldsymbol{x}_N} \end{pmatrix} \\
&\boldsymbol{U}^{*T}(\boldsymbol{k}) = (\mathrm{e}^{-i\boldsymbol{k}\cdot\boldsymbol{x}_1} \quad \mathrm{e}^{-i\boldsymbol{k}\cdot\boldsymbol{x}_2} \quad \cdots \quad \mathrm{e}^{-i\boldsymbol{k}\cdot\boldsymbol{x}_N})
\end{aligned}
\tag{7.3-4b}
$$

and $\boldsymbol{S}(\omega)$ is the cross power spectral density function matrix defined by

$$\boldsymbol{S}(\omega) = \boldsymbol{F}(\omega)\boldsymbol{F}^{*T}(\omega)$$

$$= \begin{pmatrix} F_1(\omega) \\ F_2(\omega) \\ \vdots \\ F_N(\omega) \end{pmatrix} (F_1^*(\omega) \quad F_2^*(\omega) \quad \cdots \quad F_N^*(\omega))$$

$$= \begin{pmatrix} S_{11}(\omega) & S_{12}(\omega) & \cdots & S_{1N}(\omega) \\ S_{21}(\omega) & S_{22}(\omega) & \cdots & S_{2N}(\omega) \\ \vdots & \vdots & \ddots & \vdots \\ S_{N1}(\omega) & S_{N2}(\omega) & \cdots & S_{NN}(\omega) \end{pmatrix} \tag{7.3-4c}$$

By the definition, $\boldsymbol{S}(\omega)$ is the Hermitian matrix.

Now the conventional estimation of power spectral density function is obtained as follows, by using the wight $W_n = 1/N$,

$$S_{T\boldsymbol{L}}^C(\boldsymbol{k},\omega) = \frac{1}{(2\pi)^3 L_x L_y T N^2} \left| \boldsymbol{U}^{*T}(\boldsymbol{k}) \boldsymbol{S}(\omega) \boldsymbol{U}(\boldsymbol{k}) \right| \tag{7.3-5}$$

(2) High Resolution Method

This method proposed by Capon (1969, 1973) uses the different weight $W_n(\boldsymbol{k},\omega) \equiv W_n(\omega)$ as a function of frequency wave number from the conventional method. To show the derivation of this method, the power spectral density function $S_{T\boldsymbol{L}}(\boldsymbol{k},\omega)$ given by Eq. (7.3-4a) is rewritten as,

$$S_{T\boldsymbol{L}}(\boldsymbol{k},\omega) = C\sum_{m=1}^{N}\sum_{n=1}^{N} W_m(\omega)W_n^*(\omega)F_m(\omega)F_n^*(\omega)\mathrm{e}^{-i\boldsymbol{k}\cdot(\boldsymbol{x}_m-\boldsymbol{x}_n)}$$

$$= C\sum_{m=1}^{N}\sum_{n=1}^{N} W_m(\omega)W_n^*(\omega)S_{mn}(\omega)\mathrm{e}^{-i\boldsymbol{k}\cdot(\boldsymbol{x}_m-\boldsymbol{x}_n)} \tag{7.3-6a}$$

$$= C\boldsymbol{W}^{*T}(\omega)\tilde{\boldsymbol{S}}(\omega)\boldsymbol{W}(\omega)$$

where

$$C = \frac{1}{(2\pi)^3 L_x L_y T}, \quad \tilde{S}_{mn}(\omega) = S_{mn}(\omega)\mathrm{e}^{-i\boldsymbol{k}\cdot(\boldsymbol{x}_m-\boldsymbol{x}_n)} \tag{7.3-6b}$$

The weight $W_n(\boldsymbol{k},\omega) \equiv W_n(\omega)$ is determined by the satisfying the following two conditions;

$$\text{(a)}\ \ \boldsymbol{k} \neq \boldsymbol{k}_0 : \quad \mathrm{Min}(\boldsymbol{W}^{*T}(\omega)\tilde{\boldsymbol{S}}(\omega)\boldsymbol{W}(\omega)) \tag{7.3-7a}$$

$$\text{(b)}\ \ \boldsymbol{k} = \boldsymbol{k}_0 : \quad \sum_{n=1}^{N} W_n(\boldsymbol{k}_0,\omega)F_b(\omega) = F_b(\omega) \rightarrow \boldsymbol{1}^T\boldsymbol{W}(\omega) = 1 \tag{7.3-7b}$$

where $\boldsymbol{k}_0$ is the wave number vector of the direction of wave propagation and $F_b(\omega)$ is the Fourier spectrum of the beam formed signal $f_b(t)$ obtained by the weighted delay and sum beamformer method (Capon (1969, 1973), Harada and Motohashi (2021)).

By employing the method of Lagrange multiplier, the weight satisfying Eqs. (7.3-7a) and (7.3-7b) can be obtained by minimizing the Lagrange function as follows:

$$L(\boldsymbol{W}) = \sum_{m=1}^{N}\sum_{n=1}^{N}\tilde{S}_{mn}(\omega)W_m^*(\omega)W_n(\omega) - \lambda\left(\sum_{m=1}^{N}W_m^*(\omega) - 1\right)$$

$$= \boldsymbol{W}^{*T}(\omega)\tilde{\boldsymbol{S}}(\omega)\boldsymbol{W}(\omega) - \lambda(\boldsymbol{1}^T\boldsymbol{W}^*(\omega) - 1) \tag{7.3-8a}$$

and

$$\frac{\partial L(\boldsymbol{W})}{\partial W_l^*} = 0 \tag{7.3-8b}$$

In Eq. (7.3-8a) we use the relationship that the condition given by Eq. (7.3-7b) is also written as $\boldsymbol{1}^T\boldsymbol{W}^*(\omega) = 1$ for complex conjugate weight.

From Eqs. (7.3-8a) and (7.3-8b), the weight can be obtained as follows.

$$\frac{\partial L(\boldsymbol{W})}{\partial W_l^*} = \sum_{m=1}^{N}\sum_{n=1}^{N}\tilde{S}_{mn}\left(\frac{\partial W_m^*}{\partial W_l^*}W_n\right) - \lambda\left(\sum_{n=1}^{N}\frac{\partial W_m^*}{\partial W_l^*}\right)$$

$$= \sum_{n=1}^{N}(\tilde{S}_{ln}W_n) - \lambda \tag{7.3-9a}$$

$$= \tilde{\boldsymbol{S}}(\omega)\boldsymbol{W}(\omega) - \boldsymbol{1}\lambda = 0 \rightarrow \boldsymbol{W}(\omega) = \tilde{\boldsymbol{S}}^{-1}(\omega)\boldsymbol{1}\lambda$$

In deriving the righthand side of Eq. (7.3-9a), we use the relationship as follows.

$$\frac{\partial W_m^*}{\partial W_l^*} = \begin{cases} 1 & m = l \\ 0 & m \neq l \end{cases} \tag{7.3-9b}$$

Substitution of the weight obtained in the last term of Eq. (7.3-9a) into Eq. (7.3-7b) yields the unknown parameter as

$$\lambda = (\boldsymbol{1}^T\tilde{\boldsymbol{S}}^{-1}(\omega)\boldsymbol{1})^{-1} \tag{7.3-9c}$$

It is noted here that $\boldsymbol{1}^T\tilde{\boldsymbol{S}}^{-1}(\omega)\boldsymbol{1}$ is a scalar quantity.

From Eqs. (7.3-9a) and (7.3-9c), the optimal weight is obtained such as

$$\begin{aligned}\boldsymbol{W}_{opt}(\omega) &= \tilde{\boldsymbol{S}}^{-1}(\omega)\boldsymbol{1}\lambda \\ &= (\tilde{\boldsymbol{S}}^{-1}(\omega)\boldsymbol{1})(\boldsymbol{1}^T\tilde{\boldsymbol{S}}^{-1}(\omega)\boldsymbol{1})^{-1}\end{aligned} \tag{7.3-10a}$$

When we represent the element of the inverse of power spectral density function matrix $\tilde{\boldsymbol{S}}^{-1}(\omega)$ as $\tilde{q}_{mn}(\omega)$, then Eq. (7.3-10a) can be expressed such as

$$W_{nopt}(\omega) = \frac{\sum_{m=1}^{N}\tilde{q}_{mn}(\omega)}{\sum_{m=1}^{N}\sum_{n=1}^{N}\tilde{q}_{mn}(\omega)} \tag{7.3-10b}$$

The above equation for the optimal weight is the same of that derived by Capon (1969, 1973).

By substituting Eq. (7.3-10a) into Eq. (7.3-6a) and taking account for the scalar quantity $\boldsymbol{1}^T\tilde{\boldsymbol{S}}^{-1}(\omega)\boldsymbol{1}$, the high resolution of frequency wave number power spectral density function can be obtained such as

$$\begin{aligned}S_{\boldsymbol{TL}}(\boldsymbol{k},\omega) &= C\boldsymbol{W}^{*T}(\omega)\tilde{\boldsymbol{S}}(\omega)\boldsymbol{W}(\omega) \\ &= C\frac{\boldsymbol{1}^T(\tilde{\boldsymbol{S}}^{*T}(\omega))^{-1}}{\boldsymbol{1}^T(\tilde{\boldsymbol{S}}^{*T}(\omega))^{-1}\boldsymbol{1}}\tilde{\boldsymbol{S}}(\omega)\frac{\tilde{\boldsymbol{S}}^{-1}(\omega)\boldsymbol{1}}{\boldsymbol{1}^T\tilde{\boldsymbol{S}}^{-1}(\omega)\boldsymbol{1}} \\ &= C(\boldsymbol{1}^T\tilde{\boldsymbol{S}}^{-1}(\omega)\boldsymbol{1})^{-1} \\ &= C(\boldsymbol{U}^{*T}(\boldsymbol{k})\boldsymbol{S}^{-1}(\omega)\boldsymbol{U}(\boldsymbol{k}))^{-1}\end{aligned} \tag{7.3-11a}$$

In deriving the above equation, we use the following relationship,

$$\boldsymbol{1}^T \tilde{\boldsymbol{S}}^{-1}(\omega)\boldsymbol{1} = \sum_{m=1}^{N}\sum_{n=1}^{N} S_{mn}^{-1}(\omega)\mathrm{e}^{-i\boldsymbol{k}\cdot(\boldsymbol{x}_m - \boldsymbol{x}_n)}$$

$$= \boldsymbol{U}^{*T}(\boldsymbol{k})\boldsymbol{S}^{-1}(\omega)\boldsymbol{U}(\boldsymbol{k}) \tag{7.3-11b}$$

From Eq. (7.3-11a), the high resolution of frequency wave number power spectral density function can be written such as

$$S_{T\boldsymbol{L}}^{HR}(\boldsymbol{k},\omega) = \frac{1}{(2\pi)^3 L_x L_y T}(|\,\boldsymbol{U}^{*T}(\boldsymbol{k})\boldsymbol{S}^{-1}(\omega)\boldsymbol{U}(\boldsymbol{k})\,|)^{-1} \tag{7.3-12}$$

8. SUMMARY

A new version of the simulation equations for bi-variate two-dimensional stochastic processes is described which is consistent with the spectral representation of homogeneous stational stochastic fields. The new version is taken account for the concept of quadrant symmetry. Also, the characterization of bi-variate spatially two-dimensional time-space stochastic processes is presented with a numerical example based on the analysis of seismic array records in Taiwan (SMART-1). Finally, the essentials for estimating the power spectral density function of bi-variate two-dimensional stochastic processes from a set of measured data in finite regions are presented. Also, the estimation method of the frequency wave number power spectral density function from the seismic array records.

For simplicity in this study, we discuss bi-variate one-dimensional processes, bi-variate two-dimensional processes and bi-variate spatially two-dimensional time-space processes. However, the results may be easily extended to multi-variate multi-dimensional processes by following the same procedures as those used in this study. In fact, Shinozuka (1987) presented the simulation equations for the multi-variate multi-dimensional processes.

9. ACKNOWLEDGEMENT

This work was supported by the Tokyo Gas Co., Ltd., Tokyo, Japan. The authors gratefully acknowledge the above support.

REFERENCES

1. Bendat, J.S. and Piersol, A.G. (1971): Random data: Analysis and measurement procedures, Wiley.
2. Bolt, B.A. et al. (1982): Preliminary report on the SMART-1 strong motion array in Taiwan, Report No. EERC-82/13, University of California, Berkeley.
3. Capon, J. (1969): High-resolution frequency wave number spectrum analysis, Proc. of IEEE, Vol. 57, pp.1408-1418.
4. Capon, J. (1973): Signal processing and frequency wave number spectrum analysis for a large aperture seismic array, in Methods of Computational Physics, Vol. 13, pp.1-59, Academic Press.
5. Harada, T. and Oda, T. (1985): Probabilistic analysis of seismic array data with application to lifeline earthquake engineering, Memoirs of the Faculty of Engineering, Miyazaki University, No. 15.
6. Harada, T. and Shinozuka, M. (1986, 2021): On the correlation scale

of stochastic fields, 1st and 2nd edition, Academic Repository, University of Miyazaki, http://hdl.handle.net/10458/5788

7. Harada, T. and Motohashi, H. (2020): Fourier Transform and application~Analysis of seismic ground motion, random wave fields and simulation method~, Gendaitosho Company, https://www.gendaitosho.co.jp/.

8. Shinozuka, M. and Jan, C-M. (1972): Digital simulation of random processes and its applications, Journal of Sound and Vibration, Vol. 25, No. 1, pp.111-128.

9. Shinozuka, M. (1987): Stochastic fields and their digital simulation, Stochastic Methods in Structural Dynamics, Edited by Schueller, G.I. and Shinozuka, M., Martinus Nijhoff Publishers.

10. Yaglom, A.M. (1962,1973): An introduction to the theory of stationary random functions, Prentice Hall Englewood Cliffs (1962), Dover (1973).